SYMBIONT THERMAL HISTORY AND SENSITIVITY INFORM PHOTOCHEMICAL PERFORMANCE IN THE SEA ANEMONE *EXAIPTASIA DIAPHANA* DURING ACUTE HEATING

by

Willa Mari Lane

A thesis submitted to the Faculty of the University of Delaware in partial fulfillment of the requirements for the degree of Honors Degree in Marine Science with Distinction

Spring 2023

SYMBIONT THERMAL HISTORY AND SENSITIVITY INFORM PHOTOCHEMICAL PERFORMANCE IN THE SEA ANEMONE *EXAIPTASIA DIAPHANA* DURING ACUTE HEATING

by

Willa Mari Lane

Approved: 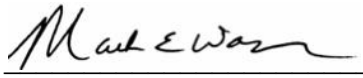

Mark E. Warner, Ph.D.
Professor in charge of thesis on behalf of the Advisory Committee

Approved: 

Mi-Ling Li, Sc.D.
Committee member from the School of Marine Science and Policy

Approved: 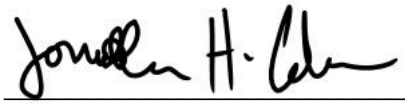

Jonathan H. Cohen, Ph.D.
Committee member from the Board of Senior Thesis Readers

Approved: _____

Michael Chajes, Ph.D
Dean, University Honors Program

ACKNOWLEDGMENTS

I am indebted to Mark Warner for making this thesis possible. Without his support, trust, and understanding, I would not have been able to complete this work. I would also like to give special thanks to my committee members, Mi-Ling Li and Jon Cohen, for their feedback and encouragement, and to other members of the Warner Lab for their help and time, especially Tim Bateman, Jess Capista, and Liz Roros. Thank you as well to Helene Intraub, who supported my exploration of one of the many other different and beautiful forms science can take; Ray Peters and Kristin Bennighoff, who saw the best in me; and Joanna York, who kept me in one piece throughout my undergraduate degree.

It is with sincere gratitude that I also recognize the funding sources and scholarships that have supported me and this thesis. These include an Honors Enrichment Award and a Harward Munson Fellowship from the University of Delaware's Honors College as well as an Ernest F. Hollings Undergraduate Scholarship from the National Oceanic and Atmospheric Administration.

Finally, thank you to my parents, Holly and Daniel Lane, for their unconditional love and support; Scott Goldberg and Gretchen Johnson, for always believing that I could (and would), and for many games of Wingspan; Zenab Khan, for always bringing humor to situations that desperately needed it; and my community in Lewes, Newark, and beyond.

TABLE OF CONTENTS

LIST OF TABLES

LIST OF FIGURES

ABSTRACT

Increasing seawater temperature due to global climate change is one of the largest threats to coral reefs. Excess heating often results in the host expelling the symbiotic algae, leading to a phenomenon commonly called coral bleaching. However, in some symbioses, these algae have the capacity to adjust to heating and can modulate this stress response. I examined how two genotypes of the symbiotic dinoflagellate *Breviolum minutum* responded to acute heat stress in the sea anemone *Exaiptasia diaphana*. Two phenotypes were tested for each genotype, one of which was thermally tolerant and previously exposed to gradual heating in free-living culture, and the other of which was thermally sensitive (i.e., wild-type) and naïve to heating. Anemones were acclimated to two different light levels to determine if photoacclimation differed by symbiont type, and if photoacclimation and symbiont type interacted to change the heat stress response. Anemones were then exposed to six hours of acute heating (from 24°C to 28, 32, 34, and 36°C), followed by a 16-hour recovery period at 28°C. At the end of acute heating, the maximum quantum yield of photosystem II (F_v/F_m) decreased with increasing temperature for all groups, but thermally selected algae exhibited less decline at low light levels. By the end of the recovery period, anemones exposed to 34°C showed some recovery in photochemistry, while F_v/F_m remained low in anemones exposed to 36°C. While F_v/F_m was sensitive to short-term heating, symbiont density and chlorophyll concentration remained similar to control values, and animal-based reactive oxygen species production did not increase with temperature. Overall, thermally selected symbionts did confer some tolerance to the host, and acute heat stress may predict the overall

thermal tolerance of host-symbiont pairings. However, both the particular response variables and the time at which they are measured are critical for accurately determining short-term thermal responses in this symbiosis.

INTRODUCTION

Corals are the best-known members of a group of marine invertebrates which form symbiotic relationships with dinoflagellate algae belonging to the family Symbiodiniaceae (LaJeunesse et al. 2018). In these symbiotic partnerships, the host provides the algae with nutrients and carbon dioxide in return for a substantial portion of the algae's energy-rich photosynthetic products, which support up to 90% of the host's daily metabolic needs in high-light environments (Falkowski et al. 1993; Dubinsky & Falkowski 2011). However, corals may bleach, that is, expel or lose their symbiotic algae, under stressful conditions. Stressors commonly implicated in bleaching are elevated sea surface temperatures—the threshold for bleaching is around 31-32°C—and high solar radiation (Weis 2008). Bleaching events are worsening, with an estimated 71% of the world's coral reefs experiencing a bleaching event between 1985 and 2017 and worldwide coral reef cover declining more than 50% from estimated 1950s baselines (Eddy et al. 2021; Virgen-Urcelay & Donner 2023). Bleaching events will continue increasing in frequency and severity as the effects of climate change are more fully realized (Spalding & Brown 2015).

While the exact cellular mechanisms of bleaching are not fully understood, some details are clear when placed in the context of each symbiotic partner as well as the stressors that induce bleaching. For the algae, heat and light stress disrupt photochemistry and induce photoinhibition, leading to lower Rubisco activity, damage to photosystem II (PSII) reaction centers and thylakoid membranes, and elevated reactive oxygen species (ROS) production that may cascade into the host (Jones et al. 1998; Warner et al. 1999; Downs et al. 2013). Notably, ROS production is heavily implicated as a mechanistic cause of coral bleaching (Downs et al. 2002; Weis 2008;

Suggett & Smith 2019), but causal evidence is inconsistent (Nielsen et al. 2018; Szabó et al. 2020). In addition to the consequences of photochemical breakdown in the algal symbiont, from a host perspective, heat and light stress can directly damage host mitochondrial membranes and induce ROS production (Dykens et al. 1992; Nii & Muscatine 1997; Weis 2008). This activates a host immune response, which may cause the host to treat the symbiont as a parasite that must be expelled (Dunn et al. 2002; Weis 2008). While there is no single agreed-upon pathway of algal expulsion, *in-situ* host-mediated symbiont degradation as well as host cell exocytosis, apoptosis, autophagy, and necrosis have all been observed (Dunn et al. 2002; Ainsworth & Hoegh-Guldberg 2008; Szabó et al. 2020). Moreover, while temperature and light stress are each capable of inducing bleaching on their own through different mechanisms (Le Tissier & Brown 1996; Downs et al. 2013; Tolleter et al. 2013), there may be additive or synergistic effects when both stressors are present (e.g. Coles & Jokiel 1978; Sinutok et al. 2022). Long-term acclimatization to high light *reduces* susceptibility to thermal stress in some corals (Dunne & Brown 2001), but short-term exposure to high light without acclimatization often results in more severe bleaching (Warner & Suggett 2016; Berg et al. 2020), and thermal stress can lower the irradiance at which photoinhibition is induced (Bhagooli & Hidaka 2004).

Photochemistry, specifically the PSII maximum quantum yield (F_v/F_m), has become a standard metric for measuring coral bleaching (McLachlan et al. 2020). F_v/F_m, a measure of overall photosynthetic efficiency and photochemical health, is nondestructively measured by active chlorophyll a fluorescence. It is rapidly downregulated during photoinhibition but recovers within hours in the absence of permanent photodamage, which typically only occurs at higher temperatures and

irradiances (Warner et al. 1996; Warner et al. 1999; Jones et al. 2000; Jones and Hoegh-Guldberg 2001; Werner et al. 2002). F_v/F_m is also potentially diagnostic of overall thermal tolerance under non-stressed conditions (Nitschke et al. 2018). Common destructive metrics of bleaching include symbiont cell density and chlorophyll a concentration. Loss in symbiont cell density is one of the simplest proxies for bleaching, but often occurs over longer timescales (days) as it is the "endpoint" of bleaching stress (Cunning & Baker 2013; Hillyer et al. 2016). Chlorophyll a, on a per-cell basis, also responds over the course of days (MacIntyre et al. 2000); it has been observed both increasing (Jones 1997) and decreasing (Rodrigues & Grottoli 2006) during bleaching, suggesting that the bleaching response of chlorophyll a and other photosynthetic pigments may be species-specific (Venn et al. 2006)

The timescale over which bleaching is assessed also matters. Many classic coral bleaching and heat stress experiments are based on chronic heating protocols which elevate and hold water temperature for weeks to months. However, given the cost and time needed for such experimental designs, acute rapid-heating protocols lasting hours to days are becoming increasingly popular as a cost-effective alternative (Grottoli et al. 2020). Many recent acute heat stress experiments have used Coral Bleaching Automated Stress Systems (CBASS), which are low-cost, simple heating/cooling systems that are easily deployed in remote field locations and capable of rapid heating and holding set water temperatures to within 0.5 °C (Voolstra et al. 2020; Evensen et al. 2021; Evensen et al. in press). Acute experiments mimic the rapid swings in temperature experienced by corals in shallow-water settings (Green et al. 2019), but do not necessarily mimic large-scale natural bleaching events occurring

over several weeks (Lesser 2007). Temperatures that are sublethal in acute experiments may be lethal in chronic experiments, and dependent variables that respond over longer timescales cannot be accurately measured in acute experiments, especially those that occur over weeks to years such as calcification. Additionally, transcriptomically measured heat stress response may vary between acute and chronic heating at temperatures ≤ 32°C as well as between test species (Savary et al. 2021). Therefore, several questions are important when considering chronic vs. acute experimental designs, including how response variables relate between chronic and acute experiments and what they possibly tell us about *in-situ* thermal resilience (Grottoli et al. 2020; Evensen et al. in press). Initial work has confirmed that, as in chronic heating experiments, patterns in F_v/F_m accurately reflect coral thermal tolerance and bleaching resilience when measured during acute heating to higher temperatures (34–38°C) for less time (six hours) than used in chronic heating experiments (Voolstra et al. 2020; Evensen et al. 2021).

Reef corals that experience larger thermal ranges may demonstrate thermal tolerance due to both short-term acclimatization and long-term adaptation of the animal, but they also host species of Symbiodiniaceae with greater thermal tolerance (Palumbi et al. 2014). Symbiotic algae are likely more capable of rapid local adaptation than host corals due to large symbiont population sizes, genetic isolation, and asexual reproduction, all of which can lead to higher rates of random somatic mutations (van Oppen et al. 2011; Howells et al. 2012; Reusch & Boyd 2013; Bateman 2022). For example, in a 30cm *Acropora millepora* colony, as many as 780 to 78,000 beneficial somatic mutations may have been acquired by the symbiont since coral settlement (van Oppen et al. 2011). While host-symbiont interactions can be

complex and unpredictable (Abrego et al. 2009; Bateman 2022), and combined stress tolerance may be tightly linked to host environment (Mieog et al. 2009; Howells et al. 2012; Hoadley et al. 2019; Hoadley et al. 2021), in many coral species, host thermal tolerance is conferred by symbiont thermal tolerance (e.g., Berkelmans & van Oppen 2006; Fisher et al. 2012; Moffat 2021) and host tolerance has been linked to symbiont local adaptation and phenotypic variation (Howells et al. 2012; Hoadley et al. 2021).

The sea anemone *Exaiptasia diaphana* is frequently used as a tractable model to study cnidarian-dinoflagellate symbioses because it is easy to maintain and to render aposymbiotic for re-infection with different strains of Symbiodiniaceae (Matthews et al. 2016; Moffat 2021; Bateman 2022). To examine the influence of algal thermal tolerance on host thermal tolerance, Bateman (2022) established thermally tolerant phenotypes of two genotypes of the symbiotic alga *Breviolum minutum* (referred to as G1 and G2 hereafter) by shifting them into progressively higher temperatures over 80 generations. These thermally tolerant phenotypes developed maximum fitness and upper thermal limits at 32°C (G1) and 31°C (G2) while free-living in culture. However, thermal tolerance in culture did not match thermal response *in hospite* in *E. diaphana*. For the G1 symbiont, both thermally selected (TS) and wild-type (WT) phenotypes supported broad thermal tolerance *in hospite* as measured by photochemical efficiency, while G2 TS symbionts outperformed G2 WT symbionts. Other response variables, including symbiont density and cellular chlorophyll a, did not change with heating *in hospite* for either algal genotype (Bateman 2022).

This thesis builds on the findings of Bateman (2022) in two key ways. First, I measured how *E. diaphana* hosting these genotypes and phenotypes of *B. minutum*

responded to low vs. high light acclimation prior to temperature stress. The muted thermal response noted by Bateman (2022) may have been due to symbiont acclimation to low light *in hospite*, and there may be as-yet unexamined tradeoffs between thermal tolerance and photoacclimation at high irradiances. Second, I examined whether acute heating can be used to determine photochemical and physiological responses to environmental stress on a short-term scale in *E. diaphana*, and if the timing of sampling matters. Prior work has demonstrated that transcriptomic response varies between measurements taken immediately post-heating and measurements taken after an 18 h recovery period (Savary et al. 2021), and it is possible that photochemical and physiological responses may also vary over a similar time period.

I hypothesized that 1) prior to heating, anemones would differentially acclimate to two light levels based on the thermal phenotype (WT vs. TS cells) and algal genotype (G1 vs. G2); 2) anemone heat stress response would match the results of Bateman (2022), with G1 anemones having higher thermal tolerance than G2 anemones, and with G2 TS anemone performing better than G2 WT anemones but G1 anemones performing similarly regardless of phenotype; 3) high light-acclimated anemones would have a stronger bleaching response than low light-acclimated anemones; and 4) the timing of sampling—either immediately post-heating or after a 16 h recovery period—would influence the response of dependent variables that respond quickly, such as F_v/F_m, but not the response of slower-responding variables, such as symbiont cell density and chlorophyll a concentration.

MATERIALS AND METHODS

Anemone infection and experimental design

Exaiptasia diaphana was originally collected in Florida and was rendered aposymbiotic by menthol exposure and maintained in the dark for > 2 years. Anemones were infected with symbiotic algae from one of two *Breviolum minutum* genotypes (designated hereafter as G1 and G2). Each genotype consisted of two phenotypes, designated as either a wild-type (WT) or a previously established thermally selected (TS) strain. These strains were developed through a 'ratchet-design' heating experiment designed to test algal growth to sequentially higher temperatures over numerous generations (Bateman 2022). The WT strain for each genotype was held at the maintenance temperature of 28°C, and the G1-TS alga maintained positive growth up to 32°C while the G2-TS alga maintained positive growth up to 31°C (Bateman 2022). These cultures were held at their respective high temperatures for 80 generations prior to any experimental work, and subsequently grown at these temperatures for an additional year.

Due to limited culture space and a broken incubator, both heat-acclimated strains were grown at 31°C for another year prior to use in this current project. Subcultures of each TS strain were then shifted to 28°C at a rate of 1°C week^{-1} and maintained at 28°C for one month prior to anemone infection. During anemone infection, algal samples from both TS and WT cultures were provided to aposymbiotic anemones twice a week with live brine shrimp for four weeks (Davy et al. 1997). Anemones were maintained in artificial seawater (34 ± 1 ‰) under cool white LED lights providing ~80 µmol photons m^{-2} s^{-1}, as measured with a cosine LI-190R

Quantum Sensor (LI-COR, Nebraska, USA), on a 12:12-hour light-dark cycle. The room temperature was 24°C and anemones were fed weekly with live brine shrimp.

After infection, anemones were subdivided into experimental treatment groups (n=4–6) and maintained in glass bowls. Each bowl was acclimated to one of two light treatments under full-spectrum, dimmable, 165 W aquarium lights (GalaxyHydro, Shenzen, China). Low-light (LL) anemones were exposed to a downwelling light of ~80 µmol photons m^{-2} s^{-1}, while high-light (HL) anemones were exposed to a weekly increase of ~50 µmol photons m^{-2} s^{-1} until reaching the final downwelling light level of ~220 µmol photons m^{-2} s^{-1}. All anemones acclimated to the final light levels for at least two weeks prior to experimental use. Anemones were fed weekly and then starved for at least seven days prior to experimental use to prevent artificially high data for anemone soluble protein measurements (described below).

My experimental design was as follows: 2 genotypes (G1 or G2) × 2 phenotypes, i.e., thermal sensitivities (TS or WT) × 2 light acclimation levels (low light, LL, or high light, HL) × 4 temperatures (28°C, 32°C, 34°C, or 36°C) × 2 sampling timepoints (immediately post-heating, or after a ~16 hour "recovery period"). Response variables were photochemical efficiency (F_v/F_m and F_q'/F_m'), symbiont cell density, chlorophyll a concentration $cell^{-1}$, and anemone intracellular ROS production. Experimental methods were validated prior to use with a pilot study on anemones hosting the native symbiont (details provided below). Acute short-term heat stress assays were conducted using Coral Bleaching Automated Stress Systems (CBASS) running on an Arduino MEGA 2560 controller (Arduino, Chiasso, Switzerland) designed to control two 250 W titanium heaters and four Peltier-type chillers (IceProbe, Nova Tec, California, USA) based on real-time temperature

feedback from wired thermistor probes. Two small aquarium pumps (Sicce Micra Plus 90 GPH, Sicce, Italy) were used to circulate water within each CBASS enclosure. Anemones were held in glass bowls covered with an additional bowl to prevent excess movement from the water mixing. This CBASS water jacket configuration was validated prior to experiments, and temperature within each bowl lagged slightly behind the CBASS temperature profile by no more than 10 minutes and differed by less than ±0.5°C from the target temperature. An error in the CBASS heater connection led the 36-HL-TS anemones to experience a temperature drop from ~36.5°C to ~35.5°C for 20 minutes.

During heat stress assays, the water temperature was raised for 3 h by linear heating from 24°C to the maximum temperature (28, 32, 34, or 36°C), and then held for another 3 h "hold" period at the set temperature. At the end of the heating phase, the temperature was lowered over 1 h back to 28°C (Fig. 1). Half of the anemones in each experimental group were removed immediately at the end of the heating phase test for photochemical and physiological responses including reactive oxygen species (ROS) production, while the remaining anemones were held in the CBASS at 28°C for 16 h more to test for differences after a recovery interval. Due to sample costs and processing time, recovery anemones were not sampled for ROS production.

Heat stress assays were performed in eight runs using two CBASS enclosures each time, with two of the four temperatures for a given phenotype tested during each run. During an experimental run, 2 to 4 bowls were placed in each CBASS. Water temperature was continuously recorded every 5 minutes in each CBASS with temperature loggers (Pro V3, HOBO, Nebraska, USA). The "control" temperature was considered to be 28°C, although this was an increase from the ambient room

temperature of 24-25°C. During each CBASS run, anemones were held under the same light intensity and cycle that they were acclimated to prior to heating. The entire heating interval occurred during the light period.

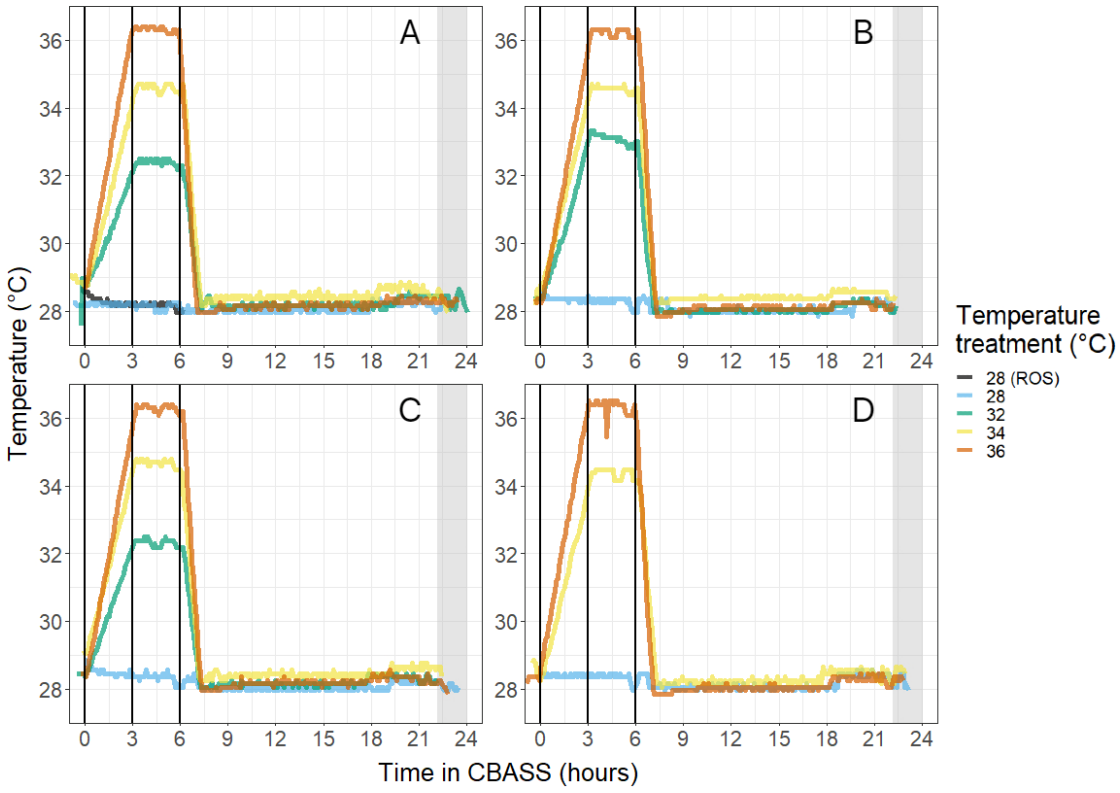

Figure 1 CBASS temperature profiles for each experimental run: A) LL WT; B) LL TS; C) HL WT; and D) HL TS. The vertical lines show the start of heating (0 h), the start of the hold period (3 h), and the end of the hold period (6 h). The grey band shows the end of the recovery period (~16 h).

For each anemone, the dark-acclimated maximum quantum yield of photosystem II (PSII) (F_v/F_m) and the light-acclimated maximum quantum yield of PSII (F_q'/F_m') were measured directly before heating, 6 h into the CBASS heating

protocol (at the end of the 3 h hold), and at the end of the 16 h recovery period with a diving pulse amplitude modulation (PAM) fluorometer (Walz, Effeltrich Germany) (Ralph et al. 1999; Robison and Warner 2006; Voolstra et al. 2020). Anemones were dark acclimated for approximately 20 minutes prior to F_v/F_m measurements. F_q'/F_m' measurements were taken directly after F_v/F_m measurements, and therefore likely do not represent the light-acclimated photochemical state for the algae. After fluorescence measurements, based on visual assessment of size, anemones were homogenized in 400 to 800 µL of phosphate buffer (50 mmol l^{-1} KH_2PO_4, 1 mmol l^{-1} EDTA, pH 7.8) with three stainless steel beads in a bead-beater (FastPrep®-24, M.P. Bio, California, USA) for 60 to 120 s at 5 m s^{-1}. For each anemone, 100 µL of homogenate was combined with 5 µL of 8% glutaraldehyde and stored at 4°C for symbiont cell density measurement. Algal cells were quantified by light microscopy at 40x magnification with replicate (n=6) counts using an improved Neubauer hemocytometer, then cell densities were normalized to anemone protein content. The remaining homogenate was aliquoted into ≤ 200 µL portions and centrifuged for 5 min at 14,000 to 16,000 rpm to pellet the symbiotic algae. Algal pellets were stored at -80°C for no more than 10 days before processing for chlorophyll a. For ROS measurements, 150 µL of animal supernatant was removed and processed as described below. All remaining animal supernatant was stored at -80°C for no more than 10 days before processing for soluble protein content.

Chlorophyll a was quantified by lysing algal pellets in 250 µL of 100% methanol with glass microbeads in a bead-beater for 60 s at 5 m s^{-1}. Methanol extracts were incubated at 4°C overnight or at -80°C for 1 to 4 days and then centrifuged for 5 m at 14,000 to 16,000 rpm to remove remaining cell debris. Extract absorbance was

measured from a 200 µL sample at 630, 664, and 750 nm on a microplate reader (Fluostar Omega, BMG, North Carolina, USA). Chlorophyll a concentration was calculated using established equations (Ritchie 2006; Bateman 2022). When possible, technical replicates (n=2) were averaged. Host protein content was determined with a modified Bradford method with a standard curve constructed using Bovine Serum Albumin (Bradford 1976; Zor and Seliger 1996; Bateman 2022). All samples and standards were measured in triplicate. 10 µL of each sample and standard was added to a 96-well microplate with 200 µL of Bradford reagent and incubated in the dark for 10 minutes, then read at 469 and 595 nm on a microplate reader.

Intracellular anemone ROS was measured at the end of the CBASS heating phase. After photochemical measurements but prior to processing, anemones were placed in individual 2 ml screw-cap tubes and incubated with 5 µM CellROX Green (ThermoFisher, Massachusetts, USA), a cell-permeable fluorogenic probe which fluoresces bright green upon binding to DNA after ROS oxidation, in CBASS seawater for 2 h in the dark at hold temperatures (Cziesielski et al. 2018; Bateman 2022). Therefore, post-heating anemones experienced 5 h of maximum treatment temperature, while recovery anemones only experienced 3 h of maximum temperature. After the 2 h incubation, anemones were washed once in phosphate buffer then processed as normal. 150 µl of animal supernatant was loaded into a black 96-well plate, and sample fluorescence intensity was measured at 468 nm excitation and 520 nm emission on a microplate reader. Fluorescence intensity was normalized to host protein content.

Prior to experimental trials, all experimental methods were validated with *E. diaphana* hosting the native symbiont (*Symbiodinium* A4) and acclimated to cool

white LED light at ~80 µmol photons m^{-2} s^{-1}. Significant differences between anemones exposed to 28°C and 36°C of heating were noted for F_v/F_m and F_q'/F_m' at the post-heating and at recovery intervals, as well as in cells µg $protein^{-1}$ at recovery. There were no differences in cells µg $protein^{-1}$ post-heating, ROS µg $protein^{-1}$ post-heating (not measured at recovery), or chl $cell^{-1}$ at either timepoint.

Deviations from experimental design

The ROS assay for all 28-LL-WT anemones was done incorrectly the first time, so an experimental trial to the post-heating timepoint was run for a second group of 28-LL-WT anemones (Fig. 1A). All data from the original group of anemones was replaced. Due to a technical software failure, the temperature of the 32°C-HL-TS CBASS treatment reached 35°C for at least an hour, so this experimental group was dropped from the analyses and is not shown in the results (Fig. 1D). Due to a water salinity issue, the G2 32-LL-TS and G1 34-LL-TS groups were removed from the experimental design. Given these omissions, there was no direct phenotype comparison for the groups in the 32-LL-WT treatments and thus these groups were also excluded from further analyses. Due to a fluorometer software error, the recovery G2 36-HL-WT anemone F_q'/F_m' recovery data was lost.

Statistical analysis

Data were visualized and analyzed in R (R Core Team, 2022, v.4.2.2) using RStudio (RStudio Team, 2022, v.2022.12.0) and packages including dplyr (Wickham et al. 2023), ggplot2 (Wickham et al. 2023), readxl (Wickham & Bryan 2022), rstatix (Kassambara 2023), magrittr (Bache & Wickham 2022), car (Fox & Weisberg 2019), and ARTool (Kay et al. 2021). Data were assessed for normality using a Shapiro-Wilk

test, homoscedasticity using Q-Q plots, and homogeneity of variance using a Levene test. Data that violated assumptions were transformed accordingly (as indicated in Appendix B) and retested; non-parametric aligned ranks analysis of variance (ANOVA) tests were used where indicated when violations to parametric tests were not resolved by data transformations.

F_v/F_m and F_q'/F_m' prior to heating were compared within each algal genotype by a two-way analysis of variance (ANOVA), with light acclimation and phenotype as factors. Genotypes were added as an additional factor in three-way ANOVA tests. Post-heating and recovery photochemistry were not directly compared since these measurements were taken at different times. For a given timepoint, each genotype and light acclimation level was considered separately for post-heating and recovery F_v/F_m, cells ug protein^{-1}, and pg chlorophyll cell^{-1}. All of these variables were assessed using two-way ANOVA tests with temperature and phenotype as factors. Light acclimation level was added as an additional factor in three-way ANOVA tests for comparing F_v/F_m between genotypes at both the post-heating and recovery timepoints.

RESULTS

Prior to heating, F_v/F_m was the same in G1 anemones regardless of phenotype and light acclimation (Fig. 2A, B). In contrast, in G2 anemones, the WT F_v/F_m was slightly but significantly higher than the TS F_v/F_m ($p<0.001$), and the HL F_v/F_m was slightly but significantly higher than the LL F_v/F_m ($p=0.047$) (Fig. 2C, D; Table S1). When comparing algal genotypes, at LL, F_v/F_m was higher in G1 anemones than G2 anemones (Fig. 2A, C), but at HL, F_v/F_m was lower in G1 anemones than G2 anemones (Fig. 2 B, D) ($p=0.030$, light acclimation × genotype; Table S2). F_v/F_m also differed by phenotype between the two genotypes ($p<0.001$, phenotype × genotype; Table S2), with F_v/F_m of 0.48 in both G1 TS and G2 WT anemones, F_v/F_m of 0.47 in G1 WT anemones, and F_v/F_m of 0.45 in G2 TS anemones. F_q'/F_m' values followed the same patterns.

Immediately after 6 h of acute heating, F_v/F_m decreased as temperature increased for all anemones (Fig. 3; $p<0.001$ for all genotype × light acclimation combinations; Tables 1, S3). In LL anemones, regardless of algal genotype, F_v/F_m decreased more rapidly in the WT anemones than in the TS anemones as temperature increased (Fig. 3A, C; $p=0.002$, phenotype × temperature; Table S4). Additionally, F_v/F_m declined faster in G2 LL anemones than G1 LL anemones overall, but G2 F_v/F_m leveled out at 36°C while G1 F_v/F_m continued to decline (Fig. 3A, C; $p=0.029$, genotype × temperature; Table S4). For G1 LL WT anemones, F_v/F_m decreased linearly with temperature, but for G1 LL TS anemones, F_v/F_m plateaued between 32°C and 34°C before dropping again (Fig. 3A). For G2 LL WT anemones, F_v/F_m decreased linearly until leveling out at 36°C, but for G2 LL TS anemones, F_v/F_m consistently decreased with temperature even at higher temperatures (Fig. 3C).

In HL anemones after 6 h of acute heating, F_v/F_m was higher in G1 anemones than G2 anemones at 28°C and 34°C, but lower in G1 anemones than G2 anemones at 36°C (Fig. 3B, D; p=0.005, temperature × genotype; Table S4). Phenotype did not matter at HL (p=0.285, temperature × phenotype; Table S4). The lack of phenotypic variation with temperature in F_v/F_m in HL anemones stands in contrast to the clear protective effect of LL TS symbionts at 34°C, especially in G1 anemones. At 34°C, TS F_v/F_m outperformed WT F_v/F_m by 174% in G1 LL anemones and by 139% in G2 LL anemones, but TS F_v/F_m was only 103% of WT F_v/F_m in G1 HL anemones and 86% in G2 HL anemones (Fig. 3; Table 1; Fig. S4). While TS anemones demonstrated a protective effect at 34°C in LL anemones, F_v/F_m was lowest for all groups at 36°C and TS anemones did not consistently outperform WT anemones at either light level (Fig. 3). F_q'/F_m' followed the same general post-heating patterns as F_v/F_m.

Immediately post-heating, F_v/F_m was 77-90% of control F_v/F_m at 32°C, 46-81% at 34°C, and 20-54% at 36°C (Table 1; Fig. S4). Contrastingly, at recovery, F_v/F_m was 83-101% of control F_v/F_m at 32°C, 79-103% at 34°C, and 30-72% at 36°C (Table 1; Fig. S4). While F_v/F_m recovered at all temperatures, recovery was clearly better at 32°C and 34°C than at 36°C (Fig. 4; p<0.001 for all genotype × light acclimation combinations; Tables S5, S6). In LL at recovery, F_v/F_m was higher in G1 than G2 anemones (Fig. 4A, C; p=0.012; Table S6). Additionally, G1 LL TS anemones outperformed G1 LL WT anemones, but G2 LL phenotypes performed similarly (Fig. 4A, C; p=0.008, genotype × phenotype; Table S6). In HL at recovery, for both genotypes, TS anemones had lower F_v/F_m values than WT anemones at 28°C and 34°C but higher values at 36°C (p=0.007; phenotype × temperature; Table S6), a result

largely driven by phenotypic differences in G2 anemones. Once again, F_q'/F_m' followed the same general patterns as F_v/F_m at recovery.

Symbiont density varied widely within and between experimental groups at the recovery timepoint (Table S7). In G1 LL WT anemones, cell density declined as temperature increased, while in G1 LL TS anemones, algal numbers remained similar until declining at 36°C (Fig. 5A; p=0.006, temperature × phenotype; Table S7). In G2 LL anemones at recovery, there was no evidence of cell loss with heating (Fig. 5C). In G1 HL anemones at recovery, while cell density declined at 34°C for both phenotypes relative to the control, there was no cell loss at 36°C (Fig. 5B). In G2 HL anemones at recovery, cell density did not significantly decline as temperature increased (Fig. 5D). High levels of variability and lack of cell loss with heating were also present post-heating (Fig. S1). Chlorophyll a concentration remained the same regardless of temperature, phenotype, or light level, and was low in all treatments at both timepoints (Fig. 6; Fig. S2; Table S8). ROS production varied widely within each experimental group, and there was no clear pattern in ROS production according to phenotype or temperature (Fig. S3). Notably, ROS production did not increase at higher temperatures.

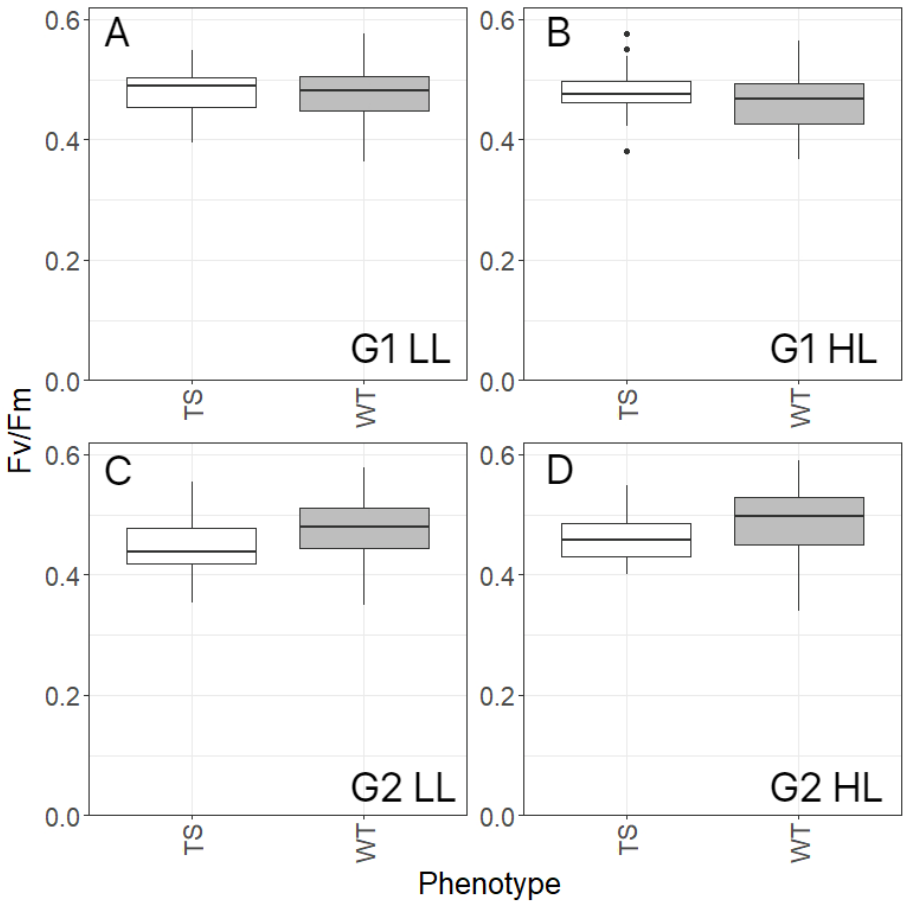

Figure 2 Maximum PSII quantum yield, F_v/F_m, of *E. diaphana* containing one of two genotypes of *B. minutum*, each of which were previously adapted to high (TS) or control (WT) temperatures and acclimated to low (LL; panes A, C) or high (HL; panes B, D) light intensity. F_v/F_m differed by phenotype between the two genotypes ($p<0.001$): while G1 phenotypes were similar ($p=0.133$; panes A, B), F_v/F_m was higher in G2 WT than G2 TS anemones ($p<0.001$; panes C, D).

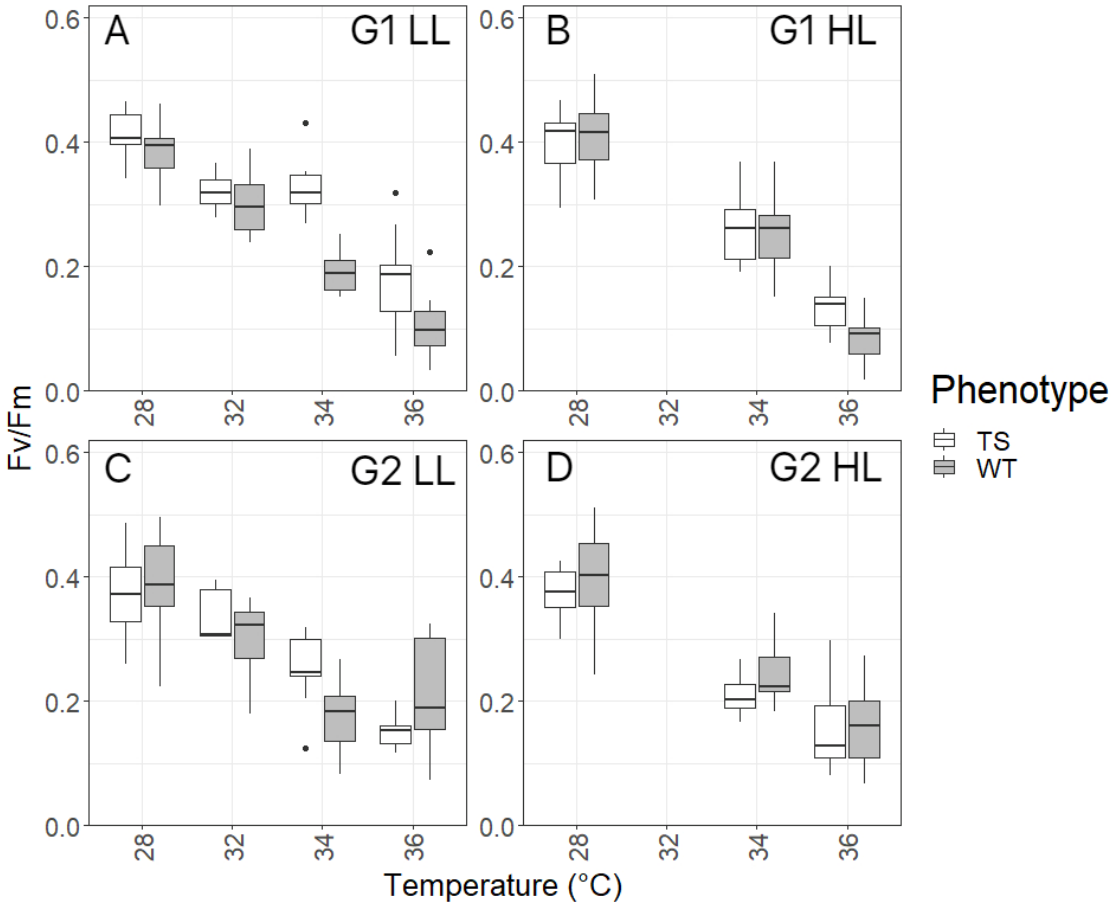

Figure 3 Maximum PSII quantum yield, F_v/F_m, of *E. diaphana* immediately after 6 h exposure to 28–36°C. Symbionts were one of two genotypes (G1 or G2) of *B. minutum* previously adapted at high (TS) or control (WT) temperatures, and acclimated to low (LL; panes A, C) or high (HL; panes B, D) light intensity. F_v/F_m decreased as temperature increased for all anemones ($p<0.001$), but declined more rapidly in LL WT than LL TS anemones ($p=0.002$; panes A, C).

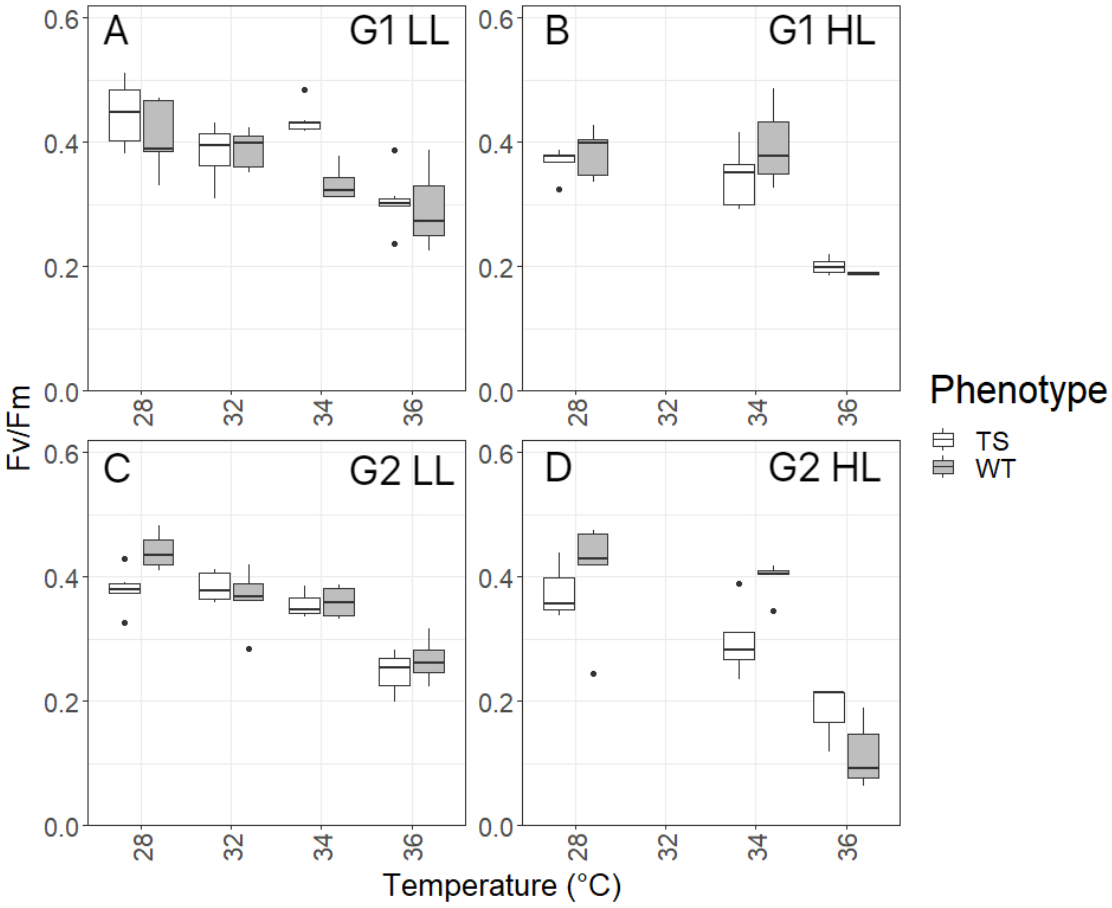

Figure 4 Maximum PSII quantum yield, F_v/F_m, of *E. diaphana* after 16 h of recovery at 28°C following 6 h exposure to 28–36°C. Each pane is presented as in Figure 3. Recovery differed by phenotype in G1 anemones at both light levels (p=0.025 for LL and 0.029 for HL; panes A, B) and by phenotype according to temperature in G2 HL anemones (p=0.045; pane D).

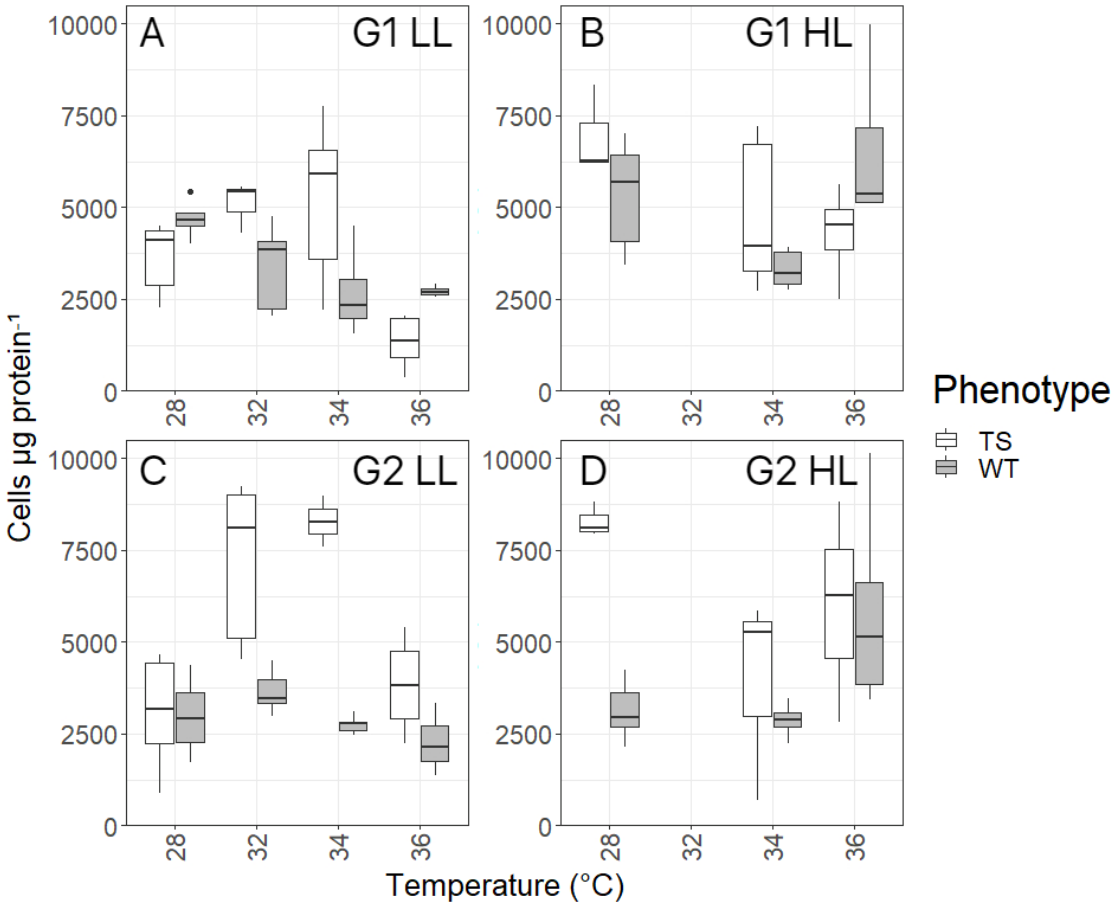

Figure 5 Symbiont cell density of *E. diaphana* after 16 h of recovery at 28°C following exposure to 28–36 °C for 6 h. Each pane is presented as in Figure 3. Symbiont cell density only significantly declined with increased temperature in G1 LL anemones (p=0.006; pane A).

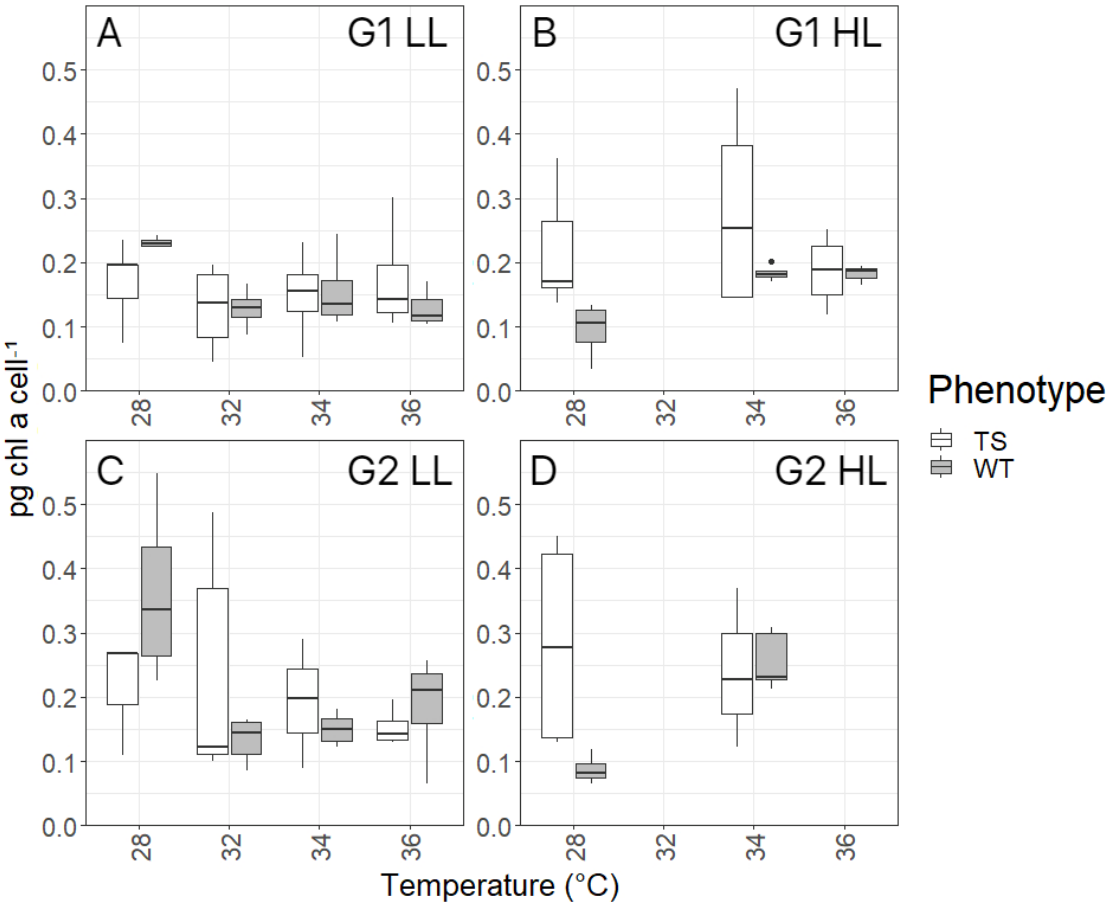

Figure 6 Chlorophyll a concentration of *B. minutum* inside of *E. diaphana* after 16 h of recovery at 28°C following exposure to 28–36°C for 6 h. Each pane is presented as in Figure 3. Chlorophyll a concentration was low in all treatments and did not decrease with heating.

Table 1 Mean F_v/F_m expressed as a percentage of mean control F_v/F_m, which standardizes comparisons across groups. The control F_v/F_m was the same genotype, light acclimation, and phenotype at 28°C for each timepoint. Post-heating anemones were compared to post-heating controls, and recovery anemones were compared to recovery controls. This data is represented visually in Figure S4.

Genotype, light acclimation, and phenotype		Maximum Temperature					
		32°C		34°C		36°C	
		Post-heating	After 16 h recovery	Post-heating	After 16 h recovery	Post-heating	After 16 h recovery
G1 LL	WT	78	95	49	82	27	72
	TS	78	86	81	98	42	69
G2 LL	WT	77	83	46	82	54	60
	TS	90	101	67	94	40	64
G1 HL	WT	-	-	61	103	20	50
	TS	-	-	65	94	34	55
G2 HL	WT	-	-	61	97	40	30
	TS	-	-	56	79	43	48

DISCUSSION

As in other studies that have examined acute heating in reef corals, photosystem II activity was the variable most responsive to heating, while other metrics presented mixed results. In general, F_v/F_m measured immediately post-heating declined with increasing temperature. While after 16 h of recovery, F_v/F_m increased in all groups, LL anemones exposed to lower temperatures—i.e., the least stressful conditions—recovered especially well. There was a breakpoint for recovery at 36°C in both LL and HL anemones, which represented the point at which PSII reaction centers were permanently damaged by acute heating. Symbiont thermal history and sensitivity and symbiont genotype interacted to inform F_v/F_m response to heating at both timepoints. I proposed four hypotheses at the outset of this research. First, I thought that prior to heating, anemones would differentially acclimate to two light levels based on thermal phenotype and algal genotype. While anemones did differentially acclimate as measured by F_v/F_m, with G2 WT anemones outperforming G2 TS anemones, there were not differences in photoacclimation based on symbiont density or chlorophyll a. Second, I thought that anemone heat stress results would match the results of Bateman (2022); the symbionts in my anemones performed similarly to symbionts in culture but not *in hospite*, likely due to the small size of my anemones. Third, I thought that HL anemones would have a stronger bleaching response than LL anemones, which was true for anemones hosting TS but not WT symbionts. Finally, I thought that timing of sampling would matter for F_v/F_m but not other variables, which was indeed the case.

Typical F_v/F_m values for healthy microalgae measured by PAM fluorescence are in the range of ~0.4-0.65 (Warner & Lesser 2010), and mean F_v/F_m values in this study ranged from 0.444–0.490 prior to heating, so true photochemical differences due

to light acclimation were likely minimal. However, prior to heating, G2 WT anemones had a slightly higher mean F_v/F_m than G2 TS anemones in both LL and HL, and F_v/F_m was also slightly but significantly higher in HL than LL in G2 anemones. In culture, G2 TS algae increased both gross and net photoinhibition rates to combat thermal stress, which manifested as a permanent phenotypical change even at 28°C, but these algae did not increase carbon fixation to support photorepair (Bateman 2022). This suggests that G2 TS cells minimized thermal stress by decreasing the number of active PSII reaction centers, which also manifested as a decline in F_v/F_m (Warner & Suggett 2016; Bateman 2022). However, this may be costly at lower temperatures because there is less machinery to carry out photosynthesis. In contrast, G1 anemones showed no difference in F_v/F_m by phenotype prior to heating. In culture, G1 TS cells increased carbon fixation while reducing reliance on photoinhibition and photorepair to combat thermal stress (Bateman 2022). Because this mechanism is more concerned with the *rate* of photosynthesis rather than the physiology of the photosynthetic machinery at high temperatures, it follows that G1 TS cells would perform similarly to G1 WT cells at room temperature. Based on photochemistry, I conclude that anemones do differentially acclimate to light levels based on symbiont genotype and thermal phenotype, but that differences are small and are not reflected in physiological measurements of chlorophyll a concentration or symbiont cell density.

When exposed to short-term acute heat stress, F_v/F_m in LL WT anemones declined more rapidly than in LL TS anemones, and LL TS anemones had notably higher F_v/F_m than LL WT anemones when exposed to 34°C. However, this heating tolerance was lost in thermally selected symbionts in heated HL anemones, as F_v/F_m was similar between both groups of TS and WT anemones at 36°C. I suggest that TS

symbionts confer some thermal tolerance to the host, that this tolerance is most obvious at 34°C, and that high irradiance can mute this tolerance. While heating to 36°C was still sublethal, several anemones were visibly stressed, retracting tentacles and sloughing tissue. At 36°C, thermal damage was likely indiscriminate regardless of phenotypic adaptations to thermal stress for each symbiont-anemone pairing. In contrast, thermal selection minimized thermal damage at 34°C in LL. However, genotypes used different strategies to minimize damage, which may explain why F_v/F_m declined faster in G2 anemones than G1 anemones at both light acclimation levels during thermal stress: G1 anemones increased photosynthesis (maybe by increasing photosynthetic electron transport) even as PSII damage occurred, while G2 anemones relied on photoinhibition to prevent PSII damage from occurring in the first place. I further posit that the advantage of thermal tolerance was not obvious in HL anemones at 34°C because high irradiance led to photoinhibition in both groups.

F_v/F_m recovered as a function of maximum exposure temperature, with anemones at 32°C and 34°C recovering most if not all photosynthetic efficiency, while anemones at 36°C struggled. Again, this points to more severe thermal damage and a potential breaking point at 36°C, where photoinhibition is more permanent than at lower temperatures. Following recovery in LL anemones, G1 F_v/F_m was again higher than G2 F_v/F_m regardless of phenotype, but G1 TS F_v/F_m was higher than G1 WT F_v/F_m while G2 TS and WT F_v/F_m were similar. Again, while G1 TS cells in culture lowered photorepair and photoinhibition and increased carbon fixation to combat thermal stress (Bateman 2022), higher carbon fixation may have meant more energy was available for photorepair during recovery (even with the reduced photorepair rate) in G1 LL TS than G1 LL WT anemones. Contrastingly, G2 TS cells in culture did not

increase carbon fixation (Bateman 2022), so there would have been minimal energy for photorepair, which explains why G2 LL TS and G2 LL WT anemones performed similarly at recovery.

In HL anemones at recovery, TS anemones generally did worse than WT anemones at 28°C and 34°C, but better at 36°C. While this pattern was present in both G1 and G2 anemones, it was much stronger in G2 anemones. Poorer photochemical performance in G1 HL TS anemones than in G1 HL WT anemones was unsurprising, because G1 TS symbionts reduced photoinhibition to cope with heat stress (Bateman 2022). At higher irradiances where photodamage was likely more pervasive, there was lower realized repair in G1 HL TS symbionts than in G1 LL TS symbionts. In G2 HL TS symbionts, as in G2 LL TS symbionts, there was minimal energy for photorepair, and there were fewer functional PSII reaction centers than in G2 HL WT symbionts to begin with (Bateman 2022). Therefore, G2 HL TS symbionts simply did not recover as well.

Given the difference in irradiance at LL and HL conditions (~80 vs. 220 µmol photons m^{-2} s^{-1}), I expected to see large differences in chlorophyll content, and, to a lesser extent, symbiont cell density. I anticipated that HL acclimated cells would have less chlorophyll a $cell^{-1}$, but that symbiont cell density would be higher in HL acclimated partnerships, as often occurs in corals growing in shallow, high-light conditions (Fitt et al. 2000; Cohen & Dubinsky 2015). However, chlorophyll a concentration and symbiont cell density did not vary between LL and HL conditions. There was no clear difference between LL and HL anemones in the 28°C control group. Chlorophyll concentration was extremely low in all groups, with a mean value of 0.20 ± 0.17 pg $cell^{-1}$ (n=263, ± SD). In several samples, chlorophyll concentrations

were below the limit of detection, which was likely due to anemone size. Typical chlorophyll concentrations in Symbiodiniaceae *in hospite* are an order of magnitude higher (e.g., Warner et al. 1996), and *Exaiptasia* grown at ~50-100 µmol photons m^{-2} s^{-1} under cool white fluorescent lights had chlorophyll concentrations averaging 1.46 pg $cell^{-1}$ (n=36, ± SE) (Muller-Parker 1984). While my anemones were initially infected with symbionts under cool white LEDs, the aquarium LEDs used for testing photoacclimation had a larger output in the blue wavelength spectra. *Exaiptasia* is a shallow-dwelling tropical genus (Bellis et al. 2018), and some shallow-dwelling symbiotic partnerships demonstrate higher photosynthetic performance under full-spectrum light rather than blue light (Mass et al. 2010). It is likely that *E. diaphana* hosting *B. minutum* strongly photoacclimation to light heavy in blue wavelengths regardless of light intensity, and that the larger amount of blue light muted the expected photoacclimation difference between LL and HL anemones.

Symbiont density did not decrease with acute heating, but there was also considerable variance in my data likely due to anemone size and experimental error. Symbiont cell density ranged from 360 - 21000 cells µg $protein^{-1}$—nearly two orders of magnitude—with a mean value of 4700 ± 2700 cells µg $protein^{-1}$ for all anemones across all timepoints (n=272, ± SD). While low chlorophyll concentrations can be explained by spectral light quality, variability in symbiont cell density is likely a result of inconsistent anemone size and issues with the soluble protein assay. Host size can affect symbiont density and chlorophyll concentrations because host tissue attenuates light, leading larger anemones to have more symbionts and higher chlorophyll $cell^{-1}$ (personal communication, M. Warner). Anemone size varied widely in my experiment, and soluble protein measurements for each anemone varied widely

between the three technical replicates for each sample, which may have resulted from incomplete mixing of the reagents. Moreover, symbiont density in re-infected *Exaiptasia* can vary significantly during the initial 12 weeks of infection, and homologous and heterologous symbionts show different patterns of establishment and ultimate symbiont density (Starzak et al. 2014). While I began infecting anemones no later than October 12, 2022, and did not begin experimental trials until 11.5 weeks later, it is possible that symbiont cell densities were still stabilizing during the experimental trials in January 2023. Finally, while symbiont cell density is often higher in shallow, high-light conditions than in deeper, low-light conditions in certain corals (Fitt et al. 2000; Cohen & Dubinsky 2015), symbiont density did not vary with irradiance when *Exaiptasia* was grown at light levels from 45–185 μmoles m^{-2} s^{-1} provided by a tungsten halogen lamp (Muller-Parker 1985). However, direct comparison between Muller-Parker (1985) and my own work is limited due to differences in lights used and the small size of my anemones.

Chlorophyll concentration and symbiont cell density also did not consistently decline with acute heating or post-recovery. Prior work has demonstrated that chlorophyll concentration and symbiont cell density respond to heat stress over a period of days (Hillyer et al. 2016; Cunning & Baker 2013; MacIntyre et al. 2000), which means that these are not appropriate response variables for acute thermal stress experiments lasting less than 24 h. Additionally, the endpoint of bleaching is typically the loss of algal cells, and less frequently the loss of chlorophyll a $cell^{-1}$. Physiological variables measured in acute heating experiments should respond over relevant timescales. PSII repair rate (i.e., D_1 protein repair) responds to environmental variation in hours, and xanthophyll cycling (conformational changes that make pigments

photoprotective) responds in seconds to minutes, making these variables germane for acute heating experiments (MacIntyre et al. 2000). F_v/F_m, a measure of overall photosynthetic efficiency and photochemical health, also responds in minutes (Chen et al. 2021), and is discussed in detail below. A final variable that responds within relevant timescales is ROS production, as ROS production should increase within hours of extreme temperature stress (Weis 2008; Oakley et al. 2017).

Host-based reactive oxygen species (ROS) did not increase as temperature increased. While this lack of any change in ROS may have been due to some introduced error in the anemone protein measurements, LL anemones 28°C displayed some of the highest concentrations of ROS µg protein^{-1}, a finding completely opposite to established patterns of ROS production during coral bleaching (Dykens et al. 1992; Nii & Muscatine 1997; Weis 2008). The ROS probe I used, CellROX Green, is designed to be a cell-permeable fluorogenic probe and was used in a similar fashion as in Cziesielski et al. (2018) and Bateman (2022) to measure ROS production by the entire anemone. Although Cziesielski et al. found that ROS production increased with heating, my results and those of Bateman (2022) draw the use of this probe into question. Symbiont ROS production, measured by CellROX Orange, also did not increase with chronic heating in *E. diaphana* hosting an unspecified symbiont (Dungan et al. 2022). CellROX Green and CellROX Orange are both cell-permeable fluorogenic probes, and the only major differences are absorption/emission spectra and whether the reagent can be formaldehyde-fixed. In combination, these findings highlight the need for thorough analysis of specific ROS produced with heating in *Exaiptasia*, such as H_2O_2 or $^1O_2$, rather than the use of generic ROS probes.

Overall, can acute thermal stress experiments be used to predict the thermal tolerance of host-symbiont partnerships? The answer will depend on several factors. In a chronic heating experiment with *E. diaphana* hosting the same *B. minutum* genotypes and phenotypes as used here, the G1 anemones performed similarly regardless of phenotype and there was no effect long-term heating at 32°C, while F_v/F_m was higher in heated G2 TS anemones than heated G2 WT anemones (Bateman 2022). In this study, after acute heating to 34°C for six hours, TS F_v/F_m was higher than WT F_v/F_m regardless of genotype at LL, while any thermal tolerance conferred by previous thermal selection in culture was lost when anemones were acutely heated at HL. While my acute *in hospite* results do not match the chronic heating results reported by Bateman (2022), this discrepancy likely arises predominantly from the different heating protocols and from differences in photoacclimation to different types of light. However, *in hospite* F_v/F_m during acute heating in my experiment aligns with F_v/F_m of the same algal phenotypes and genotypes in culture during chronic heating (Bateman 2022), with both experiments showing that thermally selected algae have a photochemical advantage when heated at low light intensities. Whether acute heating predicts thermal tolerance may depend on whether thermal tolerance is defined as tolerance in culture or *in hospite*. Previous work has shown that F_v/F_m measured in acute heat stress experiments is a good predictor of historical thermal tolerance in the coral *Stylophora pistillata* as measured by 21 d chronic assays (Voolstra et al. 2020). Ultimately, acute heating may accurately predict thermal tolerance in some cases but not others, and thermal tolerance of a symbiont in culture may or may not transfer to the overall host-symbiont partnership and is context-dependent based on the details of the experimental design that is used. I argue that in addition to predicting overall

thermal tolerance, acute heating should be considered as a method to understand critical temperatures at which symbioses break down and especially for corals already living at their thermal limit.

Temperature and light acclimation both clearly drove bleaching response as measured by F_v/F_m in my study, with TS algae performing best under low light just below the heat stress threshold. While LL and HL anemones cannot be directly statistically compared, qualitatively, bleaching response is similar. Coral morality is determined by bleaching severity and hence the amount of experienced heat stress (Anthony et al. 2009. This mortality may arise due to the loss in the ability to recover past certain threshold temperatures such as 36°C for *E. diaphana* hosting *B. minutum* in this study. While symbiont genotype-specific traits and thermal tolerance may confer benefits to the host at temperatures just below the threshold, there is a clear breakdown in recovery beyond this threshold. The threshold temperature likely differs with symbiont-host combination and heating duration. For example, the threshold temperature is likely lower during chronic than acute heating events, but continued increases in sea surface temperatures due to anthropogenic climate change will push corals already living at their thermal limit to greater temperature stress. Hence, an acute bleaching event where temperature rises quickly to a new local maximum may significantly impair recovery. Additional compounding stressors, such as disease, overfishing, and pollution (Goldberg & Wilkinson 2004), may further lower this threshold stress level. While some corals may adapt to warming by acquiring or developing more thermally tolerant symbionts (the adaptive bleaching hypothesis, e.g., Buddemeier & Fautin 1993; Kinzie et al. 2000), and rapid local adaptation in symbionts may be one such pathway of this development, host-symbiont thermal

tolerance is ultimately determined by a combination of factors including symbiont thermal tolerance, host environment, and stress history.

REFERENCES

Abrego, D., K. E. Ulstrup, B. L. Willis, and M. J. H. van Oppen. "Species–Specific Interactions between Algal Endosymbionts and Coral Hosts Define Their Bleaching Response to Heat and Light Stress." *Proceedings of the Royal Society B: Biological Sciences* 275, no. 1648 (2008): 2273–82. https://doi.org/10.1098/rspb.2008.0180.

Ainsworth, T. D., and O. Hoegh-Guldberg. "Cellular Processes of Bleaching in the Mediterranean Coral *Oculina patagonica*." *Coral Reefs* 27, no. 3 (2008): 593–97. https://doi.org/10.1007/s00338-008-0355-x.

Anthony, K. R. N., M. O. Hoogenboom, J. A. Maynard, A. G. Grottoli, and R. Middlebrook. "Energetics Approach to Predicting Mortality Risk from Environmental Stress: A Case Study of Coral Bleaching." *Functional Ecology* 23, no. 3 (2009): 539–50. https://doi.org/10.1111/j.1365-2435.2008.01531.x.

Bache, S. M., and H. Wickham. "magrittr: A Forward-Pipe Operator for R." (2022). https://cran.r-project.org/package=magrittr.

Bateman, T. G. "Physiological Dynamics of Cnidarian-Dinoflagellate Symbioses under Climate Change." PhD diss., University of Delaware. (2022).

Bellis, E. S., R. B. Endlund, H. K. Berrios, H. A. Lessios, and D. R. Denver. "Molecular Signatures of Host Specificity Linked to Habitat Specialization in Exaiptasia Sea Anemones." *Ecology and Evolution* 8, no. 11 (2018): 5413–26. https://doi.org/10.1002/ece3.4058.

Berg, J. T., C. M. David, M. M. Gabriel, and B. Bentlage. "Fluorescence Signatures of Persistent Photosystem Damage in the Staghorn Coral *Acropora cf. pulchra* (Anthozoa: Scleractinia) during Bleaching and Recovery." *Marine Biology Research* 16, no. 8–9 (2020): 643–55. https://doi.org/10.1080/17451000.2021.1875245.

Berkelmans, R., and M. J. H. van Oppen. "The Role of Zooxanthellae in the Thermal Tolerance of Corals: A 'Nugget of Hope' for Coral Reefs in an Era of Climate Change." *Proceedings of the Royal Society B: Biological Sciences* 273, no. 1599 (2006): 2305–12. https://doi.org/10.1098/rspb.2006.3567.

Bhagooli, R., and M. Hidaka. "Photoinhibition, Bleaching Susceptibility and Mortality in Two Scleractinian Corals, *Platygyra ryukyuensis* and *Stylophora pistillata*, in Response to Thermal and Light Stresses." *Comparative Biochemistry and Physiology Part A: Molecular & Integrative Physiology* 137, no. 3 (2004): 547–55. https://doi.org/10.1016/j.cbpb.2003.11.008.

Bradford, M. M. "A Rapid and Sensitive Method for the Quantitation of Microgram Quantities of Protein Utilizing the Principle of Protein-Dye Binding." *Analytical Biochemistry* 72 (1976): 248–54. https://doi.org/10.1006/abio.1976.9999.

Buddemeier, R. W., and D. G. Fautin. "Coral Bleaching as an Adaptive Mechanism." *BioScience* 43, no. 5 (1993): 320–26. https://doi.org/10.2307/1312064.

Chen, M., G. Yin, N. Zhao, T. Gan, C. Feng, M. Gu, P. Qi, and Z. Ding. "Rapid and Sensitive Detection of Water Toxicity Based on Photosynthetic Inhibition Effect." *Toxics* 9, no. 12 (2021): 321. https://doi.org/10.3390/toxics9120321.

Cohen, I., and Z. Dubinsky. “Long term photoacclimation responses of the coral *Stylophora pistillata* to reciprocal deep to shallow transplantation: photosynthesis and calcification.” *Frontiers in Marine Science* 2 (2015): 45. https://doi.org/10.3389/fmars.2015.00045.

Coles, S. L., and P. L. Jokiel. “Synergistic Effects of Temperature, Salinity and Light on the Hermatypic Coral *Montipora verrucosa*.” *Marine Biology* 49, no. 3 (1978): 187–95. https://doi.org/10.1007/BF00391130.

Cunning, R., and A. C. Baker. “Excess Algal Symbionts Increase the Susceptibility of Reef Corals to Bleaching.” *Nature Climate Change* 3, no. 3 (2013): 259–62. https://doi.org/10.1038/nclimate1711.

Cziesielski, M. J., Y. J. Liew, G. Cui, S. Schmidt-Roach, S. Campana, C. Marondedze, and M. Aranda. “Multi-Omics Analysis of Thermal Stress Response in a Zooxanthellate Cnidarian Reveals the Importance of Associating with Thermotolerant Symbionts.” *Proceedings. Biological Sciences* 285, no. 1877 (2018): 20172654. https://doi.org/10.1098/rspb.2017.2654.

Davy, S. K., J. R. Turner, and I. A. N. Lucas. “The Nature of Temperate Anthozoan-Dinoflagellate Symbioses.” In *Proceedings of the Eighth International Coral Reef Symposium*, 2 (1997):1307–12. Balboa, Panama: Smithsonian Tropical Research Institute. http://fau.digital.flvc.org/islandora/object/fau%3A31676.

Downs, C. A., J. E. Fauth, J. C. Halas, P. Dustan, J. Bemiss, and C. M. Woodley. “Oxidative Stress and Seasonal Coral Bleaching.” *Free Radical Biology and Medicine* 33, no. 4 (2002): 533–43. https://doi.org/10.1016/S0891-5849(02)00907-3.

Downs, C. A., K. E. McDougall, C. M. Woodley, J. E. Fauth, R. H. Richmond, A. Kushmaro, S. W. Gibb, Y. Loya, G. K. Ostrander, and E. Kramarsky-Winter. “Heat-Stress and Light-Stress Induce Different Cellular Pathologies in the Symbiotic Dinoflagellate during Coral Bleaching.” *PLoS ONE* 8, no. 12 (2013): e77173. https://doi.org/10.1371/journal.pone.0077173.

Dubinsky, Z., and P. Falkowski. “Light as a Source of Information and Energy in Zooxanthellate Corals.” In *Coral Reefs: An Ecosystem in Transition*, edited by Z. Dubinsky and N. Stambler, 107–18. Springer Nature: Dordrecht, Netherlands (2011). https://doi.org/10.1007/978-94-007-0114-4_8.

Dungan, A. M., J. Maire, A. Perez-Gonzalez, L. L. Blackall, and M. J. H. van Oppen. “Lack of Evidence for the Oxidative Stress Theory of Bleaching in the Sea Anemone, *Exaiptasia diaphana*, under Elevated Temperature.” *Coral Reefs* 41, no. 4 (2022): 1161–72. https://doi.org/10.1007/s00338-022-02251-w.

Dunn, S. R., J. C. Bythell, M. D. A. Le Tissier, W. J. Burnett, and J. C. Thomason. “Programmed Cell Death and Cell Necrosis Activity during Hyperthermic Stress-Induced Bleaching of the Symbiotic Sea Anemone *Aiptasia sp.*” *Journal of Experimental Marine Biology and Ecology* 272, no. 1 (2002): 29–53. https://doi.org/10.1016/S0022-0981(02)00036-9.

Dunne, R., and B. Brown. “The Influence of Solar Radiation on Bleaching of Shallow Water Reef Corals in the Andaman Sea, 1993–1998.” *Coral Reefs* 20, no. 3 (2001): 201–10. https://doi.org/10.1007/s003380100160.

Dykens, J. A., J. M. Shick, C. Benoit, G. R. Buettner, and G. W. Winston. “Oxygen Radical Production in the Sea Anemone *Anthopleura elegantissima* and Its

Endosymbiotic Algae." *Journal of Experimental Biology* 168, no. 1 (1992): 219–41. https://doi.org/10.1242/jeb.168.1.219.
Eddy, T. D., V. W. Y. Lam, G. Reygondeau, A. M. Cisneros-Montemayor, K. Greer, M. L. D. Palomares, J. F. Bruno, Y. Ota, and W. W. L. Cheung. "Global Decline in Capacity of Coral Reefs to Provide Ecosystem Services." *One Earth* 4, no. 9 (2021): 1278–85. https://doi.org/10.1016/j.oneear.2021.08.016.
Evensen, N. R., M. Fine, G. Perna, C. R. Voolstra, and D. J. Barshis. "Remarkably High and Consistent Tolerance of a Red Sea Coral to Acute and Chronic Thermal Stress Exposures." *Limnology and Oceanography* 66, no. 5 (2021): 1718–29. https://doi.org/10.1002/lno.11715.
Evensen, N. R., K. Parker, T. Oliver, S. R. Palumbi, C. Logan, J. Ryan, C. Klepac, et al. "The Coral Bleaching Automated Stress System (CBASS): A Low Cost, Portable System for the Standardized Empirical Assessment of Coral Thermal Limits." *Limnology and Oceanography: Methods*, in press.
Falkowski, P. G., Zvy D., L. Muscatine, and L. McCloskey. "Population Control in Symbiotic Corals." *BioScience* 43, no. 9 (1993): 606–11. https://doi.org/10.2307/1312147.
Fisher, P. L., M. K. Malme, and S. Dove. "The Effect of Temperature Stress on Coral–*Symbiodinium* Associations Containing Distinct Symbiont Types." *Coral Reefs* 31, no. 2 (2012): 473–85. https://doi.org/10.1007/s00338-011-0853-0.
Fitt, W. K., F. K. McFarland, M. E. Warner, and G. C. Chilcoat. "Seasonal patterns of tissue biomass and densities of symbiotic dinoflagellates in reef corals and relation to coral bleaching." *Limnology and Oceanography* 45, no. 3 (2000): 677–685. https://doi.org/10.4319/lo.2000.45.3.0677.
Fox, J., and S. Weisberg. *An {R} Companion to Applied Regression, Third Edition*. Sage: Thousand Oaks, CA, USA (2019). https://socialsciences.mcmaster.ca/jfox/Books/Companion/.
Goldberg, J., and C. Wilkinson. "Global threats to coral reefs: coral bleaching, global climate change, disease, predator plagues, and invasive species." In *Status of Coral Reefs of the World: 2004*, edited by C. Wilkinson, 67–92. Australian Institute of Marine Science (2004). https://researchonline.jcu.edu.au/24190.
Green, R. H., R. J. Lowe, M. L. Buckley, T. Foster, and J. P. Gilmour. "Physical Mechanisms Influencing Localized Patterns of Temperature Variability and Coral Bleaching within a System of Reef Atolls." *Coral Reefs* 38, no. 4 (2019): 759–71. https://doi.org/10.1007/s00338-019-01771-2.
Grottoli, A. G., R. J. Toonen, R. van Woesik, R. Vega Thurber, M. E. Warner, R. H. McLachlan, J. T. Price, et al. "Increasing Comparability among Coral Bleaching Experiments." *Ecological Applications* 31, no. 4 (2021): e02262. https://doi.org/10.1002/eap.2262.
Hillyer, K. E., D. A. Dias, A. Lutz, S. P. Wilkinson, U. Roessner, and S. K. Davy. "Metabolite Profiling of Symbiont and Host during Thermal Stress and Bleaching in the Coral *Acropora aspera*." *Coral Reefs* 36, no. 1 (2017): 105–18. https://doi.org/10.1007/s00338-016-1508-y.
Hoadley, K. D., A. M. Lewis, D. C. Wham, D. T. Pettay, C. Grasso, R. Smith, D. W. Kemp, T. C. LaJeunesse, and M. E. Warner. "Host–Symbiont Combinations Dictate

the Photo-Physiological Response of Reef-Building Corals to Thermal Stress." *Scientific Reports* 9, no. 1 (2019): 9985. https://doi.org/10.1038/s41598-019-46412-4.
Hoadley, K. D., D. T. Pettay, A. Lewis, D. Wham, C. Grasso, R. Smith, D. W. Kemp, T. LaJeunesse, and M. E. Warner. "Different Functional Traits among Closely Related Algal Symbionts Dictate Stress Endurance for Vital Indo-Pacific Reef-Building Corals." *Global Change Biology* 27, no. 20 (2021): 5295–5309. https://doi.org/10.1111/gcb.15799.
Howells, E. J., V. H. Beltran, N. W. Larsen, L. K. Bay, B. L. Willis, and M. J. H. van Oppen. "Coral Thermal Tolerance Shaped by Local Adaptation of Photosymbionts." *Nature Climate Change* 2, no. 2 (2012): 116–20. https://doi.org/10.1038/nclimate1330.
Jones, R. J. "Changes in Zooxanthellar Densities and Chlorophyll Concentrations in Corals during and after a Bleaching Event." *Marine Ecology Progress Series* 158 (1997): 51–59. https://doi.org/10.3354/meps158051.
Jones, R. J., O. Hoegh-Guldberg, A. W. D. Larkum, and U. Schreiber. "Temperature-Induced Bleaching of Corals Begins with Impairment of the CO2 Fixation Mechanism in Zooxanthellae." *Plant, Cell & Environment* 21, no. 12 (1998): 1219–30. https://doi.org/10.1046/j.1365-3040.1998.00345.x.
Jones, R. J., S. Ward, A. Y. Amri, and O. Hoegh-Guldberg. "Changes in Quantum Efficiency of Photosystem II of Symbiotic Dinoflagellates of Corals after Heat Stress, and of Bleached Corals Sampled after the 1998 Great Barrier Reef Mass Bleaching Event." *Marine and Freshwater Research* 51, no. 1 (2000): 63–71. https://doi.org/10.1071/mf99100.
Jones, R. J, and O. Hoegh-Guldberg. "Diurnal Changes in the Photochemical Efficiency of the Symbiotic Dinoflagellates (Dinophyceae) of Corals: Photoprotection, Photoinactivation and the Relationship to Coral Bleaching." *Plant, Cell & Environment* 24, no. 1 (2001) 89–99. https://doi.org/10.1046/j.1365-3040.2001.00648.x.
Kassambara, A. "rstatix: Pipe-Friendly Framework for Basic Statistical Tests." (2023). https://cran.r-project.org/package=rstatix.
Kay, M., L. Elkin, J. Higgins, and J. Wobbrock. "ARTool: Aligned Rank Transform for Nonparametric Factorial ANOVAs." (2021). https://doi.org/10.5281/zenodo.594511.
Kinzie, R. A., M. Takayama, S. R. Santos, and M. A. Coffroth. "The Adaptive Bleaching Hypothesis: Experimental Tests of Critical Assumptions." *The Biological Bulletin* 200, no. 1 (2001): 51–58. https://doi.org/10.2307/1543084.
LaJeunesse, T. C., J. E. Parkinson, P. W. Gabrielson, H. J. Jeong, J. D. Reimer, C. R. Voolstra, and S. R. Santos. "Systematic Revision of Symbiodiniaceae Highlights the Antiquity and Diversity of Coral Endosymbionts." *Current Biology* 28, no. 16 (2018): 2570-2580.e6. https://doi.org/10.1016/j.cub.2018.07.008.
Le Tissier, M. D. A., and B. E. Brown. "Dynamics of Solar Bleaching in the Intertidal Reef Coral *Goniastrea aspera* at Ko Phuket, Thailand." *Marine Ecology Progress Series* 136, no. 1/3 (1996): 235–44. https://www.jstor.org/stable/24856737.
Lesser, M. P. "Oxidative Stress Causes Coral Bleaching during Exposure to Elevated Temperatures." *Coral Reefs* 16, no. 3 (1997): 187–92. https://doi.org/10.1007/s003380050073.

MacIntyre, H. L., T. M. Jana, and R. J. Geider. “The Effect of Water Motion on Short-Term Rates of Photosynthesis by Marine Phytoplankton.” *Trends in Plant Science* 5, no. 1 (2000): 12–17. https://doi.org/10.1016/s1360-1385(99)01504-6.

Mass, T., D. I. Kline, M. Roopin, C. J. Veal, S. Cohen, D. Iluz, and O. Levy. “The Spectral Quality of Light Is a Key Driver of Photosynthesis and Photoadaptation in *Stylophora pistillata* Colonies from Different Depths in the Red Sea.” *Journal of Experimental Biology* 213, no. 23 (2010): 4084–91. https://doi.org/10.1242/jeb.039891.

Matthews, J. L., A. E. Sproles, C. A. Oakley, A. R. Grossman, V. M. Weis, and S. K. Davy. “Menthol-Induced Bleaching Rapidly and Effectively Provides Experimental Aposymbiotic Sea Anemones (*Aiptasia sp.*) for Symbiosis Investigations.” *Journal of Experimental Biology* 219, no. 3 (2016): 306–10. https://doi.org/10.1242/jeb.128934.

McLachlan, R. H., J. T. Price, S. L. Solomon, and A. G. Grottoli. “Thirty Years of Coral Heat-Stress Experiments: A Review of Methods.” *Coral Reefs* 39, no. 4 (2020): 885–902. https://doi.org/10.1007/s00338-020-01931-9.

Mieog, J. C., J. L. Olsen, R. Berkelmans, S. A. Bleuler-Martinez, B. L. Willis, and M. J. H. van Oppen. “The Roles and Interactions of Symbiont, Host and Environment in Defining Coral Fitness.” *PLOS ONE* 4, no. 7 (2009): e6364. https://doi.org/10.1371/journal.pone.0006364.

Moffat, J. J. “Symbiont Genotype Influences Host Response to Temperature in Model Cnidarian-Dinoflagellate Mutualism.” Master’s thesis, California State University Northridge (2021).

Muller-Parker, G. “Photosynthesis-irradiance responses and photosynthetic periodicity in the sea anemone Aiptasia pulchella and its zooxanthellae.” *Marine Biology* 82 (1984): 225–232. https://doi.org/10.1007/BF00392403

Muller-Parker, G. “Effect of feeding regime and irradiance on the photophysiology of the symbiotic sea anemone Aiptasia pulchella.” *Marine Biology* 90 (1985): 65–74. https://doi.org/10.1007/BF00428216.

Neilsen, D. A., K. Petrou, and R. D. Gates. “Coral Bleaching from a Single Cell Perspective.” *The ISME Journal* 12, no. 6 (2018): 1558–67. https://doi.org/10.1038/s41396-018-0080-6.

Nii, C. M., and L. Muscatine. “Oxidative Stress in the Symbiotic Sea Anemone *Aiptasia pulchella* (Carlgren, 1943): Contribution of the Animal to Superoxide Ion Production at Elevated Temperature.” *The Biological Bulletin* 192, no. 3 (1997): 444–56. https://doi.org/10.2307/1542753.

Nitschke, M. R., S. G. Gardner, S. Goyen, L. Fujise, E. F. Camp, P. J. Ralph, and D. J. Suggett. “Utility of Photochemical Traits as Diagnostics of Thermal Tolerance amongst Great Barrier Reef Corals.” *Frontiers in Marine Science* 5 (2018): 45. https://doi.org/10.3389/fmars.2018.00045

Oakley, C. A., E. Durand, S. P. Wilkinson, L. Peng, V. M. Weis, A. R. Grossman, and S. K. Davy. “Thermal Shock Induces Host Proteostasis Disruption and Endoplasmic Reticulum Stress in the Model Symbiotic Cnidarian Aiptasia.” *Journal of Proteome Research* 16, no. 6 (2017): 2121–2134. https://doi.org/10.1021/acs.jproteome.6b00797.

Palumbi, S. R., D. J. Barshis, N. Traylor-Knowles, and R. A. Bay. “Mechanisms of Reef Coral Resistance to Future Climate Change.” *Science* 344, no. 6186 (2014): 895–98. https://doi.org/10.1126/science.1251336.

R Core Team. “R: A Language and Environment for Statistical Computing.” Vienna, Austria: R Foundation for Statistical Computing (2022). https://www.R-project.org/.

Ralph, P. J., R. Gademann, A. W. D. Larkum, and U. Schreiber. “In Situ Underwater Measurements of Photosynthetic Activity of Coral Zooxanthellae and Other Reef-Dwelling Dinoflagellate Endosymbionts.” *Marine Ecology Progress Series* 180 (1999): 139–47. https://doi.org/10.3354/meps180139.

Reusch, T. B. H., and P. W. Boyd. “Experimental Evolution Meets Marine Phytoplankton.” *Evolution; International Journal of Organic Evolution* 67, no. 7 (2013): 1849–59. https://doi.org/10.1111/evo.12035.

Ritchie, R. J. “Consistent Sets of Spectrophotometric Chlorophyll Equations for Acetone, Methanol and Ethanol Solvents.” *Photosynthesis Research* 89, no. 1 (2006): 27–41. https://doi.org/10.1007/s11120-006-9065-9.

Robison, J. D., and M. E. Warner. “Differential Impacts of Photoacclimation and Thermal Stress on the Photobiology of Four Different Phylotypes of *Symbiodinium* (Pyrrhophyta).” *Journal of Phycology* 42, no. 3 (2006): 568–79. https://doi.org/10.1111/j.1529-8817.2006.00232.x.

Rodrigues, L. J., and A. G. Grottoli. “Lipids and Chlorophyll in Bleached and Recovering *Montipora capitata* from Hawaii: An Experimental Approach.” In *Proceedings of the Eighth International Coral Reef Symposium*, 1 (2003):696–701. Okinawa, Japan: Smithsonian Tropical Research Institute. https://www.researchgate.net/profile/Andrea-Grottoli/publication/237456673_Lipids_and_chlorophyll_in_bleached_and_recovering_Montipora_capitata_from_Hawaii_An_experimental_approach/links/0f317538cbc45595fd000000/Lipids-and-chlorophyll-in-bleached-and-recovering-Montipora-capitata-from-Hawaii-An-experimental-approach.pdf

Savary, R., D. J. Barshis, C. R. Voolstra, A. Cárdenas, N. R. Evensen, G. Banc-Prandi, M. Fine, and A. Meibom. “Fast and Pervasive Transcriptomic Resilience and Acclimation of Extremely Heat-Tolerant Coral Anemones from the Northern Red Sea.” *Proceedings of the National Academy of Sciences of the United States of America* 118, no. 19 (2021): e2023298118. https://doi.org/10.1073/pnas.2023298118.

Sinutok, S., P. Chotikarn, M. S. Pattaratumrong, P. Moungkeaw, P. Pramneechote, and M. Yucharoen. “Synergistic Effect of Elevated Temperature and Light Stresses on Physiology of *Pocillopora acuta* from Different Environments.” *Journal of Marine Science and Engingeering* 10, no. 6 (2022): 790. https://doi.org/10.3390/jmse10060790.

Spalding, M. D., and B. E. Brown. “Warm-Water Coral Reefs and Climate Change.” *Science* 350, no. 6262 (2015): 769–71. https://doi.org/10.1126/science.aad0349.

Starzak, D. E., R. G. Quinnell, M. R. Nitschke, and S. K. Davy. “The influence of symbiont type on photosynthetic carbon flux in a model cnidarian–dinoflagellate symbiosis.” *Marine Biology* 161 (2014): 711–724. https://doi.org/10.1007/s00227-013-2372-8.

Suggett, D. J., and D. J. Smith. “Coral Bleaching Patterns Are the Outcome of Complex Biological and Environmental Networking.” *Global Change Biology* 26, no. 1 (2020): 68–79. https://doi.org/10.1111/gcb.14871.

Szabó, M., A. W. D. Larkum, and I. Vass. “A Review: The Role of Reactive Oxygen Species in Mass Coral Bleaching.” In *Photosynthesis in Algae: Biochemical and Physiological Mechanisms*, edited by A. W. D. Larkum, A. R. Grossman, and J. A. Raven, 459–88. Springer International Publishing (2020). https://doi.org/10.1007/978-3-030-33397-3_17.

Tolleter, D., F. O. Seneca, J. C. DeNofrio, C. J. Krediet, S. R. Palumbi, J. R. Pringle, and A. R. Grossman. “Coral Bleaching Independent of Photosynthetic Activity.” *Current Biology* 23, no. 18 (2013): 1782–86. https://doi.org/10.1016/j.cub.2013.07.041.

van Oppen, M. J. H., P. Souter, E. J. Howells, A. Heyward, and R. Berkelmans. “Novel Genetic Diversity Through Somatic Mutations: Fuel for Adaptation of Reef Corals?” *Diversity* 3, no. 3 (2011): 405–23. https://doi.org/10.3390/d3030405.

Venn, A. A., M. A. Wilson, H. G. Trapido-Rosenthal, B. J. Keely, and A. E. Douglas. “The Impact of Coral Bleaching on the Pigment Profile of the Symbiotic Alga, *Symbiodinium*.” *Plant, Cell & Environment* 29, no. 12 (2006): 2133–42. https://doi.org/10.1111/j.1365-3040.2006.001587.x.

Virgen-Urcelay, A., and S. D. Donner. “Increase in the Extent of Mass Coral Bleaching over the Past Half-Century, Based on an Updated Global Database.” *PLOS ONE* 18, no. 2 (2023): e0281719. https://doi.org/10.1371/journal.pone.0281719.

Voolstra, C. R., C. Buitrago-López, G. Perna, A. Cárdenas, B. C. C. Hume, N. Rädecker, and D. J. Barshis. “Standardized Short-term Acute Heat Stress Assays Resolve Historical Differences in Coral Thermotolerance across Microhabitat Reef Sites.” *Global Change Biology* 26, no. 8 (2020): 4328–43. https://doi.org/10.1111/gcb.15148.

Warner, M. E., W. K. Fitt, and G. W. Schmidt. “The Effects of Elevated Temperature on the Photosynthetic Efficiency of Zooxanthellae in Hospite from Four Different Species of Reef Coral: A Novel Approach.” *Plant, Cell & Environment* 19, no. 3 (1996): 291–99. https://doi.org/10.1111/j.1365-3040.1996.tb00251.x.

Warner, M. E., W. K. Fitt, and G. W. Schmidt. “Damage to Photosystem II in Symbiotic Dinoflagellates: A Determinant of Coral Bleaching.” *Proceedings of the National Academy of Sciences* 96, no. 14 (1999): 8007–12. https://doi.org/10.1073/pnas.96.14.8007.

Warner, M. E., P. J. Ralph, and M. P. Lesser. “Chlorophyll fluorescence in reef building corals.” In *Chlorophyll Fluorescence in Aquatic Sciences: Methods and Applications*, edited by D. J. Suggett, O. Prasil, & M. Borowitzka, 209–222. Springer International Publishing (2010). https://doi.org/10.1007/978-90-481-9268-7_10.

Warner, M. E., and D. J. Suggett. “The Photobiology of Symbiodinium spp.: Linking Physiological Diversity to the Implications of Stress and Resilience.” In *The Cnidaria, Past, Present and Future*, edited by S. Goffredo and Z. Dubinsky, 489–509. Springer International Publishing (2016). https://doi.org/10.1007/978-3-319-31305-4_30.

Weis, V. M. “Cellular Mechanisms of Cnidarian Bleaching: Stress Causes the Collapse of Symbiosis.” *Journal of Experimental Biology* 211, no. 19 (2008): 3059–66. https://doi.org/10.1242/jeb.009597.

Werner, C., O. Correia, and W. Beyschlag. “Characteristic patterns of chronic and dynamic photoinhibition of different functional groups in a Mediterranean ecosystem.” *Functional Plant Biology* 29, no. 8 (2002): 999–1011. https://doi.org/10.1071/PP01143.

Wickham, H., and J. Bryan. “readxl: Read Excel Files.” (2022). https://cran.r-project.org/package=readxl.
Wickham, H., W. Chang, L. Henry, T. L. Pedersen, K. Takahashi, C. Wilke, K. Woo, H. Yutani, D. Dunnington, and RStudio. “ggplot2: Elegant Graphics for Data Analysis.” (2023). https://ggplot2.tidyverse.org.
Wickham, H., R. François, L. Henry, K. Müller, and D. Vaughan. “dplyr: A Grammar of Data Manipulation.” (2023). https://dplyr.tidyverse.org.
Zor, T., and Z. Selinger. “Linearization of the Bradford Protein Assay Increases Its Sensitivity: Theoretical and Experimental Studies.” *Analytical Biochemistry* 236, no. 2 (1996): 302–8. https://doi.org/10.1006/abio.1996.0171.

Appendix A
SUPPLEMENTARY FIGURES

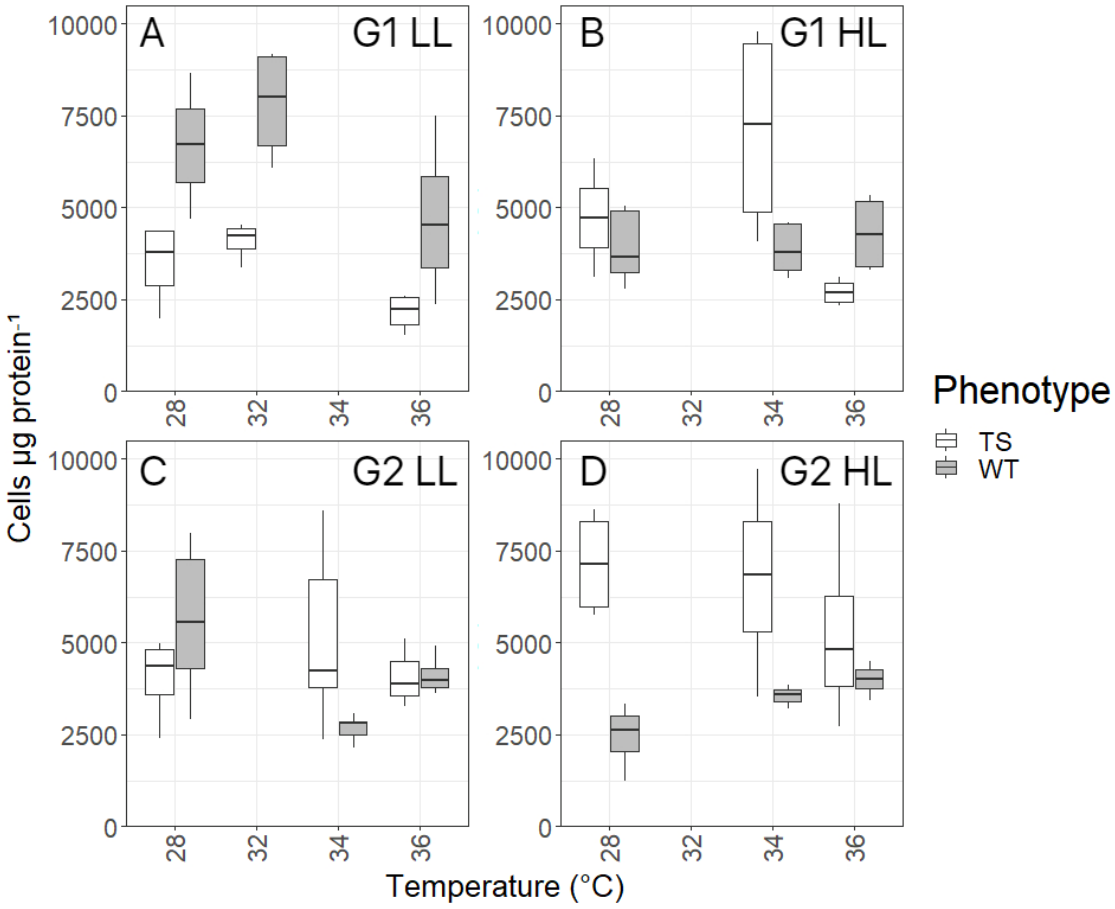

Figure S1 Symbiont cell density of *E. diaphana* after 6 h of exposure to 28–36°C. Each pane is presented as in Figure 3. Symbiont cell density did not decrease with increased temperature.

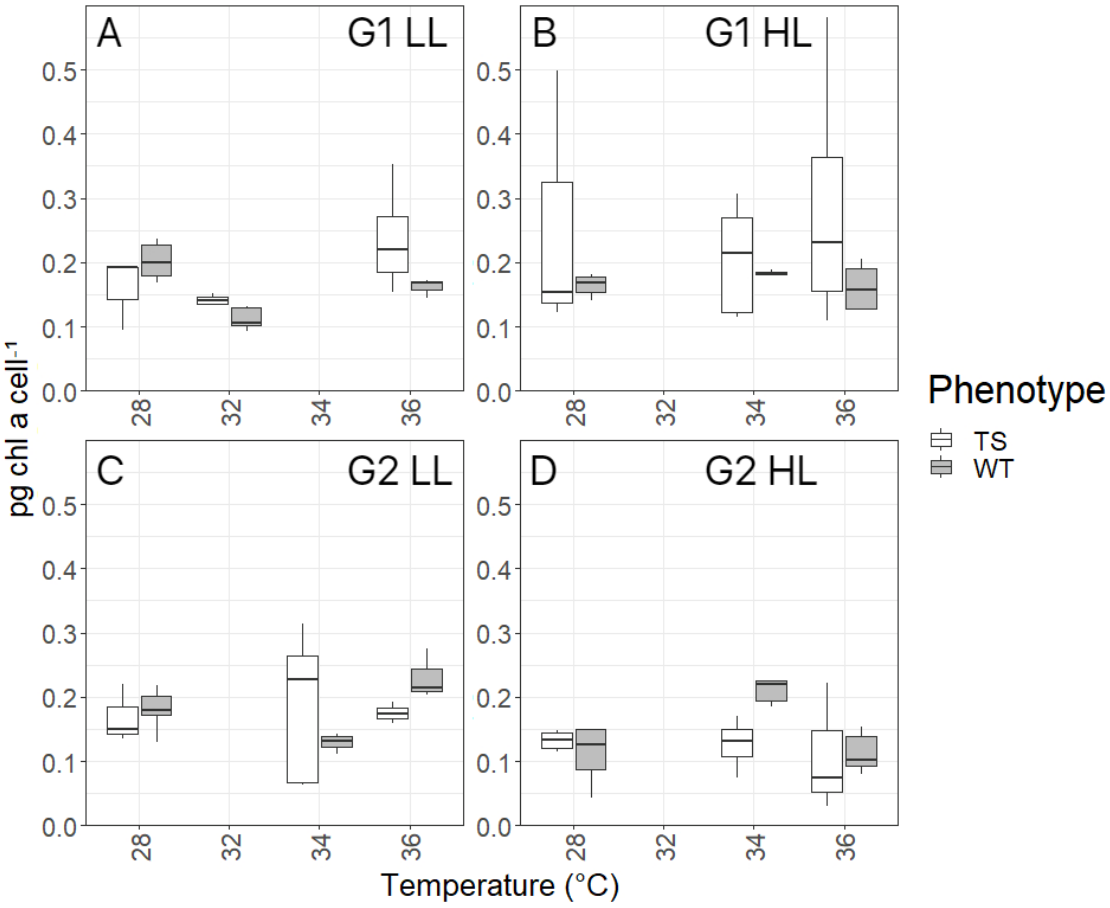

Figure S2 Chlorophyll a concentration of *B. minutum* inside of *E. diaphana* after 6 h of exposure to 28–36°C. Each pane is presented as in Figure 3. Chlorophyll a concentration was low in all treatments and did not decrease with heating.

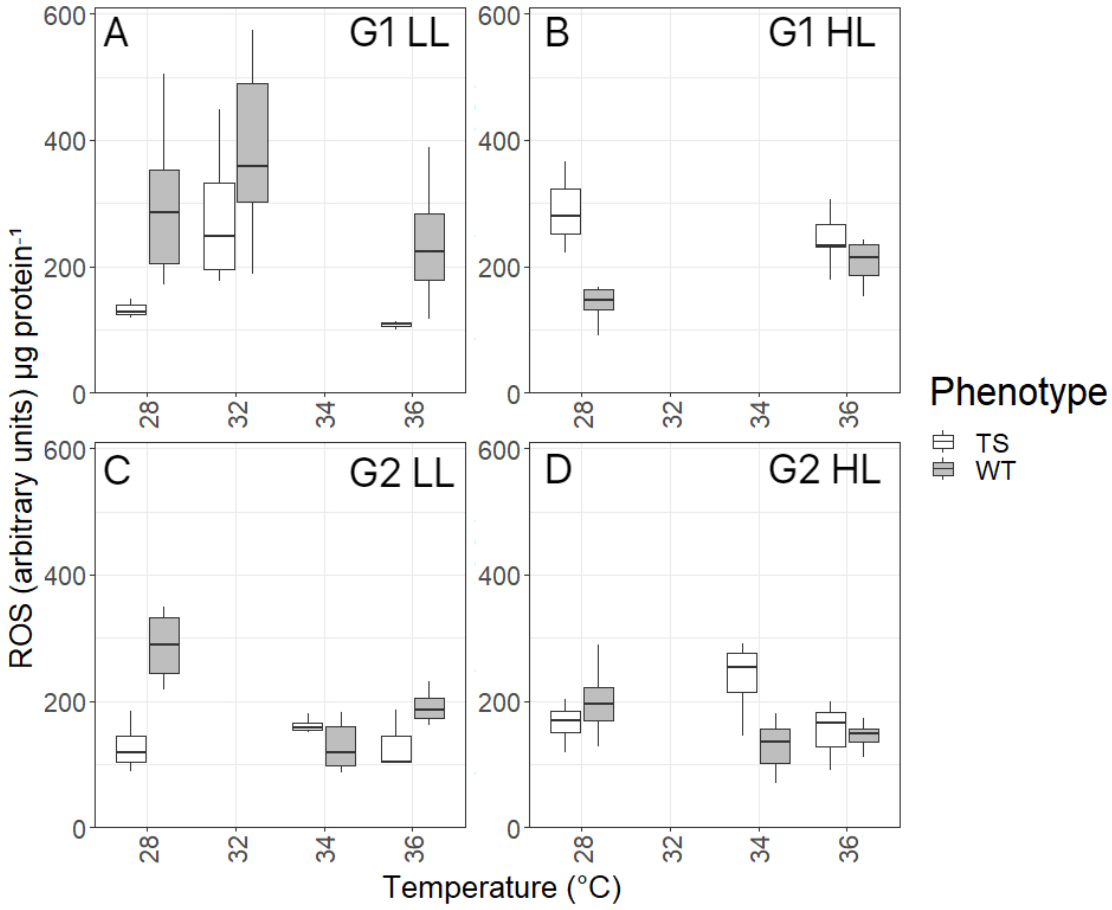

Figure S3 Intracellular ROS measured in *E. diaphana* after 8 h of exposure to 28–36°C. Each pane is presented as in Figure 3. ROS did not increase with increased temperature.

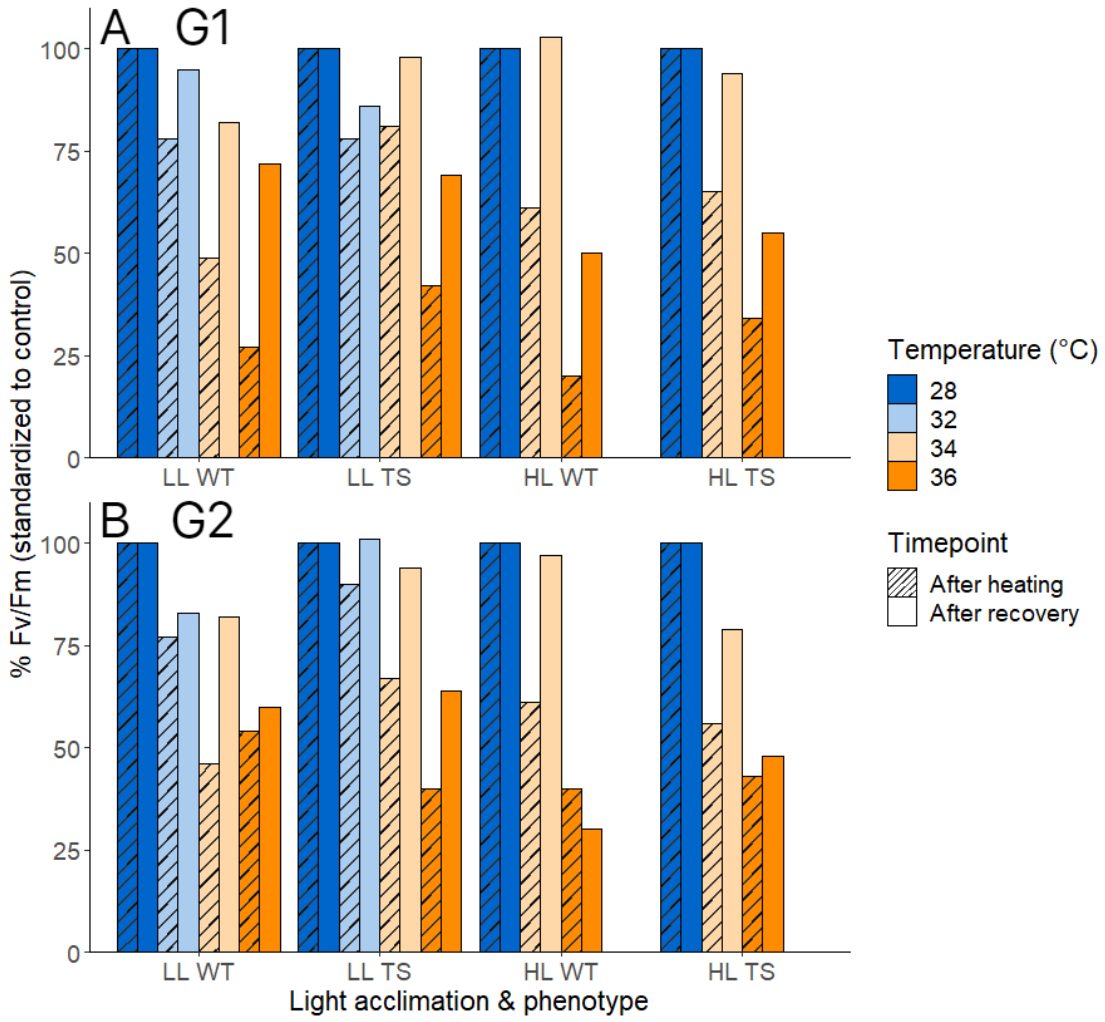

Figure S4 F_v/F_m standardized to control values in *E. diaphana* hosting symbionts of different genotypes (G1, pane A, or G2, pane B) of *B. minutum* previously adapted at high (TS) or control (WT) temperatures and acclimated to low (LL) or high (HL) light intensity. Measurements were taken after a 6 h exposure to 28–36°C or after a 16 h overnight recovery at 28°C. The control value was the same genotype, light acclimation, and phenotype at 28°C at each time point.

Appendix B
ANOVA TABLES

Table S1 Two-way analysis of variance (ANOVA) results prior to heating for dark acclimated PSII maximum quantum yield (F_v/F_m).

Genotype	Variable	df	Sum of squares	F-value	p-value	Group mean (n=)
G1	Light	1	0.002	0.820	0.367	LL = 0.477 (74) HL = 0.470 (68)
	Phenotype	1	0.004	2.288	0.133	WT = 0.468 (80) TS = 0.480 (62)
	Light × phenotype	1	0.002	0.880	0.250	LLWT = 0.474 (40) LLSS = 0.479 (34) HLWT = 0.462 (40) HLSS = 0.481 (28)
G2	*Light*	*1*	*0.001*	*4.034*	*0.047*	LL = 0.462 (78) HL = 0.479 (61)
	Phenotype	*1*	*0.028*	*11.403*	*<0.001*	WT = 0.481 (86) TS = 0.452 (53)
	Light × phenotype	1	0.000	0.000	0.989	LLWT = 0.473 (48) LLSS = 0.444 (30) HLWT = 0.490 (38) HLSS = 0.461 (23)

Table S2 Three-way analysis of variance (ANOVA) results prior to heating for dark acclimated PSII maximum quantum yield (F_v/F_m). See Table S1 for additional group means.

Variable	df	Sum of squares	F-value	p-value	Group mean (n=)
Light	1	0.002	0.822	0.365	LL = 0.469 (152) HL = 0.474 (129)
Phenotype	1	0.004	1.909	0.168	WT = 0.475 (166) TS = 0.467 (115)
Genotype	1	0.001	0.503	0.479	G1 = 0.473 (142) G2 = 0.470 (139)
Light × phenotype	1	0.001	0.430	0.512	LLWT = 0.474 (88) LLTS = 0.463 (64) HLWT = 0.476 (78) HLTS = 0.472 (51)
Light × genotype	*1*	*0.010*	*4.748*	*0.030*	G1LL = 0.477 (74) G1HL = 0.470 (68) G2LL = 0.462 (78) G2HL = 0.479 (61)
Phenotype × genotype	*1*	*0.027*	*12.443*	*< 0.001*	G1WT = 0.468 (80) G1TS = 0.480 (62) G2WT = 0.481 (86) G2TS = 0.452 (53)
Light × phenotype × genotype	1	0.001	0.362	0.548	

Table S3 Two-way analysis of variance (ANOVA) results for dark acclimated PSII maximum quantum yield (F_v/F_m) immediately after 6 h of heating.

Genotype, light level	Variable	df	Sum of squares	F-value	p-value	Group mean (n=)
G1, LL	*Temperature*	*3*	*0.624*	*73.590*	*< 0.001*	28 = 0.396 (19) 32 = 0.308 (17) 34 = 0.244 (16) 36 = 0.143 (18)
	Phenotype	*1*	*0.065*	*22.846*	*< 0.001*	WT = 0.252 (38) TS = 0.302 (32)
	Temperature × phenotype	*3*	*0.037*	*4.385*	*0.007*	28WT = 0.384 (10) 28TS = 0.410 (10) 32WT = 0.300 (10) 32TS = 0.321 (7) 34WT = 0.190 (10) 34TS = 0.332 (6) 36WT = 0.105 (8) 36TS = 0.174 (10)
G1, HL	*Temperature*	*2*	*0.855*	*147.350*	*< 0.001*	28 = 0.407 (19) 34 = 0.256 (20) 36 = 0.107 (19)
	Phenotype	1	0.002	0.981	0.327	WT = 0.245 (29) TS = 0.269 (29)
	Temperature × phenotype	2	0.010	1.744	0.185	28WT = 0.415 (9) 28TS = 0.400 (10) 34WT = 0.252 (10) 34TS = 0.260 (10) 36WT = 0.084 (10) 36 TS = 0.134 (9)
G2, LL	*Temperature*	*3*	*0.509*	*37.606*	*< 0.001*	28 = 0.381 (22) 32 = 0.310 (17) 34 = 0.209 (21) 36 = 0.187 (19)
	Phenotype	1	0.002	0.383	0.538	WT = 0.268 (48) TS = 0.282 (31)
	Temperature × phenotype	*3*	*0.044*	*3.237*	*0.027*	28WT = 0.387 (12) 28TS = 0.374 (10) 32WT = 0.299 (12) 32TS = 0.338 (5) 34WT = 0.179 (12) 34TS = 0.249 (9) 36WT = 0.208 (12) 36 TS = 0.151 (7)
G2, HL	*Temperature*	*2*	*0.482*	*59.402*	*< 0.001*	28 = 0.390 (17) 34 = 0.226 (16) 36 = 0.161 (18)
	Phenotype	1	0.005	1.199	0.279	WT = 0.270 (28) TS = 0242 (23)
	Temperature × phenotype	2	0.002	0.303	0.740	28WT = 0.400 (10) 28TS = 0.375 (7) 34WT = 0.243 (8) 34TS = 0.209 (8) 36WT = 0.161 (10) 36TS = 0.160 (8)

Table S4 Three-way analysis of variance (ANOVA) results for dark acclimated PSII maximum quantum yield (F_v/F_m) immediately after 6 h of heating. See Table S3 for additional group means.

Light level	Variable	df	Sum of squares	F-value	p-value	Group mean (n=)
LL	*Temperature*	*3*	*1.102*	*98.638*	*< 0.001*	28 = 0.388 (41) 32 = 0.309 (34) 34 = 0.224 (37) 36 = 0.166 (37)
	Phenotype	*1*	*0.036*	*9.628*	*0.002*	WT = 0.261 (86) TS = 0.292 (63)
	Genotype	1	0.000	0.005	0.943	G1 = 0.275 (70) G2 = 0.273 (79)
	Temperature × phenotype	*3*	*0.057*	*5.091*	*0.002*	28WT = 0.385 (22) 28TS = 0.391 (19) 32WT = 0.299 (22) 32TS = 0.328 (12) 34WT = 0.184 (22) 34TS = 0.282 (15) 36WT = 0.167 (20) 36TS = 0.165 (17)
	Temperature × genotype	*3*	*0.035*	*3.110*	*0.029*	28G1 = 0.396 (19) 28G2 = 0.381 (22) 32G1 = 0.308 (17) 32G2 = 0.310 (17) 34G1 = 0.244 (16) 34G2 = 0.209 (21) 36G1 = 0.143 (18) 36G2 = 0.187 (19)
	Phenotype × genotype	*1*	*0.028*	*7.561*	*0.007*	G1WT = 0.252 (38) G1TS = 0.302 (32) G2WT = 0.268 (48) G2TS = 0.282 (31)
	Temperature × phenotype × genotype	3	0.033	2.006	0.116	

Table S4 Cont.

Light level	Variable	df	Sum of squares	F-value	p-value	Group mean (n=)
HL	*Temperature*	*2*	*1.300*	*189.130*	*< 0.001*	28 = 0.399 (36) 34 = 0.243 (36) 36 = 0.133 (37)
	Phenotype	1	0.000	0.018	0.895	WT = 0.257 (52) TS = 0.257 (57)
	Genotype	1	0.000	0.049	0.825	G1 = 0.257 (58) G2 = 0.258 (51)
	Temperature × phenotype	2	0.009	1.271	0.285	28WT = 0.407 (19) 28TS = 0.390 (17) 34WT = 0.248 (18) 34TS = 0.237 (18) 36WT = 0.123 (20) 36TS = 0.146 (17)
	Temperature × genotype	*2*	*0.038*	*5.535*	*0.005*	28G1 = 0.407 (19) 28G2 = 0.390 (17) 34G1 = 0.256 (20) 34G2 = 0.226 (16) 36G1 = 0.107 (19) 36G2 = 0.161 (18)
	Phenotype × genotype	1	0.008	2.352	0.128	G1WT = 0.245 (29) G1TS = 0.269 (29) G2WT = 0.270 (28) G2TS = 0.242 (23)
	Temperature × phenotype × genotype	2	0.002	0.283	0.754	

Table S5 Two-way analysis of variance (ANOVA) results for dark acclimated PSII maximum quantum yield (F_v/F_m) after 16 h of recovery at 28°C.

Genotype, light level	Variable	df	Sum of squares	F-value	p-value	Group mean (n=)
G1, LL	*Temperature*	*3*	*0.079*	*11.331*	*< 0.001*	28 = 0.427 (10) 32 = 0.386 (9) 34 = 0.395 (10) 36 = 0.302 (9)
	Phenotype	*1*	*0.013*	*5.610*	*0.025*	WT = 0.365 (17) TS = 0.391 (21)
	Temperature × phenotype	3	0.016	2.258	0.102	28WT = 0.409 (5) 28TS = 0.445 (5) 32WT = 0.389 (5) 32TS = 0.383 (4) 34WT = 0.334 (4) 34TS = 0.436 (6) 36WT = 0.295 (3) 36TS = 0.306 (6)
G1, HL *Data did not respond to transfor-mations, so this is an Aligned Ranks ANOVA.	*Temperature*	*2*		*10.911*	*< 0.001*	28 = 0.375 (10) 34 = 0.370 (10) 36 = 0.197 (6)
	Phenotype	*1*		*5.555*	*0.029*	WT = 0.355 (12) TS = 0.312 (14)
	Temperature × phenotype	2		1.136	0.341	28WT = 0.382 (5) 28TS = 0.367 (5) 34WT = 0.395 (5) 34TS = 0.345 (5) 36WT = 0.189 (2) 36 TS = 0.201 (4)
G2, LL	*Temperature*	*3*	*0.107*	*29.953*	*< 0.001*	28 = 0.410 (12) 32 = 0.374 (10) 34 = 0.358 (8) 36 = 0.257 (7)
	Phenotype	1	0.003	2.937	0.097	WT = 0.367 (20) TS = 0.353 (17)
	Temperature × phenotype	3	0.009	2.619	0.070	28WT = 0.441 (6) 28TS = 0.380 (6) 32WT = 0.365 (5) 32TS = 0.384 (5) 34WT = 0.360 (5) 34TS = 0.356 (3) 36WT = 0.266 (4) 36TS = 0.245 (3)
G2, HL	*Temperature*	*2*	*0.305*	*38.553*	*< 0.001*	28 = 0.396 (8) 34 = 0.352 (9) 36 = 0.140 (8)
	Phenotype	1	0.004	0.937	0.345	WT = 0.306 (15) TS = 0.287 (10)
	Temperature × phenotype	*2*	*0.029*	*3.660*	*0.045*	28WT = 0.408 (5) 28TS = 0.378 (3) 34WT = 0.397 (5) 34TS = 0.297 (4) 36WT = 0.114 (5) 36TS = 0.183 (3)

Table S6 Three-way analysis of variance (ANOVA) results for dark acclimated PSII maximum quantum yield (F_v/F_m) after 16 h of recovery at 28°C. See Table S5 for additional group means.

Light level	Variable	df	Sum of squares	F-value	p-value	Group mean (n=)
LL	*Temperature*	*3*	*0.176*	*33.295*	*< 0.001*	28 = 0.418 (22) 32 = 0.380 (19) 34 = 0.379 (18) 36 = 0.283 (16)
	Phenotype	1	0.003	1.785	0.187	WT = 0.366 (37) TS = 0.374 (38)
	Genotype	*1*	*0.012*	*6.712*	*0.012*	G1 = 0.379 (38) G2 = 0.360 (37)
	Temperature × phenotype	3	0.014	2.567	0.063	28WT = 0.426 (11) 28TS = 0.410 (11) 32WT = 0.377 (10) 32TS = 0.383 (9) 34WT = 0.348 (9) 34TS = 0.409 (9) 36WT = 0.279 (7) 36TS = 0.286 (9)
	Temperature × genotype	3	0.003	0.522	0.669	28G1 = 0.427 (10) 28G2 = 0.410 (12) 32G1 = 0.386 (9) 32G2 = 0.374 (10) 34G1 = 0.395 (10) 34G2 = 0.358 (8) 36G1 = 0.302 (9) 36G2 = 0.257 (7)
	Phenotype × genotype	*1*	*0.013*	*7.483*	*0.008*	G1WT = 0.365 (17) G1TS = 0.391 (21) G2WT = 0.367 (20) G2TS = 0.353 (17)
	Temperature × phenotype × genotype	3	0.013	2.504	0.068	

Table S6 Cont.

Light level	Variable	df	Sum of squares	F-value	p-value	Group mean (n=)
HL	*Temperature*	*2*	*0.446*	*78.155*	*< 0.001*	28 = 0.384 (18) 34 = 0.361 (19) 36 = 0.164 (14)
	Phenotype	1	0.005	1.663	0.205	WT = 0.328 (27) TS = 0.301 (24)
	Genotype	1	0.004	1.345	0.253	G1 = 0.332 (26) G2 = 0.298 (25)
	Temperature × phenotype	*2*	*0.032*	*5.672*	*0.007*	28WT = 0.395 (10) 28TS = 0.371 (8) 34WT = 0.396 (10) 34TS =0.323 (9) 36WT = 0.135 (7) 36TS = 0.193 (7)
	Temperature × genotype	2	0.008	1.381	0.263	28G1 = 0.375 (10) 28G2 = 0.396 (8) 34G1 = 0.370 (10) 34G2 = 0.352 (9) 36G1 = 0.197 (6) 36G2 = 0.140 (8)
	Phenotype × genotype	1	0.000	0.106	0.747	G1WT = 0.355 (12) G1TS = 0.312 (14) G2WT = 0.306 (15) G2TS = 0.287 (10)
	Temperature × phenotype × genotype	2	0.005	0.936	0.400	

Table S7 Two-way analysis of variance (ANOVA) results for symbiont cell density (cells µg protein^{-1}) after 16 h of recovery at 28°C.

Genotype, light level	Variable	df	Sum of squares	F-value	p-value	Group mean (n=)
G1, LL	*Temperature*	*3*	*31997797*	*6.679*	*0.002*	28 = 4098 (9) 32 = 4033 (8) 34 = 4211 (10) 36 = 1849 (8)
	Phenotype	1	2208062	1.383	0.250	WT = 3415 (16) TS = 3758 (19)
	Temperature × phenotype	*3*	*24808870*	*5.178*	*0.006*	28WT = 4689 (4) 28TS = 3625 (5) 32WT = 3395 (5) 32TS = 5096 (3) 34WT = 2689 (4) 34TS = 5225 (6) 36WT = 2720 (3) 36TS = 1326 (5)
G1, HL	*Temperature*	*2*	*18463603*	*3.679*	*0.042*	28 = 5928 (8) 34 = 4043 (10) 36 = 5548 (9)
	Phenotype	1	410754	0.164	0.690	WT = 5063 (15) TS = 5153(12)
	Temperature × phenotype	*2*	*21223592*	*4.229*	*0.029*	28WT = 5323 (5) 28TS = 6937 (3) 34WT = 3312 (5) 34TS = 4774 (5) 36WT = 6555 (5) 36TS = 4289 (4)
G2, LL *Data transformed with natural log.	*Temperature*	*3*	*2.463*	*5.674*	*0.004*	28 = 3034 (9) 32 = 5425 (10) 34 = 4332 (7) 36 = 2953 (9)
	Phenotype	*1*	*2.115*	*14.617*	*0.001*	WT = 2907 (19) TS = 5201 (16)
	Temperature × phenotype	3	1.267	2.918	0.0523	28WT = 2979 (4) 28TS = 3077 (5) 32WT = 3653 (5) 32TS = 7197 (5) 34WT = 2752 (5) 34TS = 8281 (2) 36WT = 2259 (5) 36TS = 3819 (4)
G2, HL	Temperature	2	25235076	3.190	0.067	28 = 5063 (8) 34 = 3327 (7) 36 = 5890 (8)
	Phenotype	*1*	*25086749*	*6.342*	*0.022*	WT = 4026 (14) TS = 6061 (9)
	Temperature × phenotype	2	26559062	3.357	0.059	28WT = 3133 (5) 28TS = 8280 (3) 34WT = 2872 (4) 34TS = 3934 (3) 36WT = 5843 (5) 36TS = 5969 (3)

Table S8 Two-way analysis of variance (ANOVA) results for chlorophyll a concentration (pg chlorophyll a $cell^{-1}$) after 16 h of recovery at 28°C.

Genotype, light level	Variable	df	Sum of squares	F-value	p-value	Group mean (n=)
G1, LL	Temperature	3	0.017	1.478	0.246	28 = 0.192 (8) 32 = 0.128 (8) 34 = 0.152 (8) 36 = 0.157 (8)
	Phenotype	1	0.000	0.083	0.776	WT = 0.159 (14) TS = 0.157 (18)
	Temperature × phenotype	3	0.011	0.960	0.428	28WT = 0.231 (3) 28TS = 0.168 (5) 32WT = 0.128 (4) 32TS = 0.129 (4) 34WT = 0.156 (4) 34TS = 0.149 (4) 36WT = 0.130 (3) 36TS = 0.173 (5)
G1, HL *Data transformed with square root.	Temperature	2	0.036	2.390	0.115	28 = 0.166 (12) 34 = 0.237 (9) 36 = 0.185 (7)
	Phenotype	*1*	*0.062*	*8.171*	*0.009*	WT = 0.146 (12) TS = 0.229 (16)
	Temperature × phenotype	2	0.026	1.721	0.202	28WT = 0.095 (5) 28TS = 0.217 (7) 34WT = 0.183 (4) 34TS = 0.280 (5) 36WT = 0.182 (3) 36TS = 0.187 (4)
G2, LL *Data transformed with natural log.	Temperature	3	1.676	2.437	0.086	28 = 0.299 (7) 32 = 0.187 (11) 34 = 0.164 (9) 36 = 0.170 (8)
	Phenotype	1	0.0016	0.007	0.933	WT = 0.198 (16) TS = 0.202 (19)
	Temperature × phenotype	3	0.864	1.257	0.309	28WT = 0.361 (4) 28TS = 0.215 (3) 32WT = 0.134 (5) 32TS = 0.232 (6) 34WT = 0.150 (6) 34TS = 0.193 (3) 36WT = 0.186 (4) 36TS = 0.153 (4)
G2, HL *Data transformed with reciprocal.	*Temperature*	*1*	*82.794*	*13.031*	*0.003*	28 = 0.185 (8) 34 = 0.326 (9)
	Phenotype	*1*	*47.726*	*7.512*	*0.017*	WT = 0.181 (9) TS = 0.348 (8)
	Temperature × phenotype	*1*	*59.120*	*8.833*	*0.011*	28WT = 0.087 (4) 28TS = 0.284 (4) 34WT = 0.256 (5) 34TS = 0.413 (4)